5-2014

Thermal Analysis of Binding of Organic Pollutants to Titanium Dioxide

Shashidhar Annarapu
Western Kentucky University, shashidhar.annarapu965@topper.wku.edu

THERMAL ANALYSIS OF BINDING OF ORGANIC POLLUTANTS TO TITANIUM DIOXIDE

A Thesis
Presented to
The Faculty of the Department of Chemistry
Western Kentucky University
Bowling Green, Kentucky

In Partial Fulfillment
Of the Requirements for the Degree
Master of Science

By
Shashidhar Annarapu

May 2014

THERMAL ANALYSIS OF BINDING OF ORGANIC POLLUTANTS TO TITANIUM DIOXIDE

Date Recommended 4/28/2014

Dr. Matthew J. Nee, Director of Thesis

Dr. Quentin Lineberry

Dr. Bangbo Yan

4-28-14

Dean, Graduate Studies and Research Date

I want to dedicate my thesis to my parents, Annarapu Venkat Reddy, Annarapu Indira and my sister Annarapu Lalitha, who have supported me financially and mentally. Without them I would not be in the position where I am now. Also, I would like to dedicate my thesis to my research advisor, Dr. Matthew Nee, who guided me throughout my research and supported me in all ways possible.

ACKNOWLEDGMENTS

First, I would like to express my sincere gratitude to my advisor, Dr. Matthew Nee, for the extended support for the entire work. His guidance helped me in all the time of research and writing the thesis. Because of his motivation, immense knowledge, and patience, this work was done without hassles. I could not have imagined having a better advisor and mentor for my master's study. I would like to thank Dr. Quentin Lineberry for giving me the opportunity to use instruments in the Thermal Analysis Laboratory. I would also like to thank Dr. Aaron Celestian for giving training and allowing me to use the powder XRD instrument. I would like to dedicate this thesis to my parents, Annarapu Venkat Reddy and Annarapu Indira, who have given me support in all the ways possible. I thank God for my everyday life.

TABLE OF CONTENTS

LIST OF FIGURES

LIST OF TABLES

THERMAL ANALYSIS OF BINDING OF ORGANIC POLLUTANTS TO TITANIUM DIOXIDE

Shashidhar Annarapu May 2014 48 Pages

Directed by: Dr. Matthew J. Nee, Dr. Quentin Lineberry, Dr. Bangbo Yan

Department of Chemistry Western Kentucky University

Conventional waste water treatment processes are not completely effective in removing highly stable organic compounds. Photocatalytic degradation on titanium dioxide is a possible alternative technique for many classes of these compounds. Several studies have been done by other researchers to study mechanisms of photocatalytic degradation, which occurs either through direct oxidation by holes or via indirect oxidation by radical messengers. Titanium dioxide can oxidize substrates directly through hole oxidation mechanisms or indirectly through free radical mechanisms. Substrates must bind onto the catalyst surface to undergo direct oxidation by holes. Thermogravimetric analysis (TGA) was performed on four different classes of compounds; iodinated contrast agents (iohexol and diatrizoate), polycyclic aromatic hydrocarbons (perylene and pyrene), the antibacterial agent triclosan and the pesticide atrazine, to investigate which of the compounds are adsorbed on the surface of titanium dioxide to undergo direct oxidation through electron holes. Differential scanning calorimetry (DSC) was conducted on triclosan and atrazine to determine if the desorption reaction is endothermic or exothermic. Powder X-ray diffraction was performed on all four classes of compounds to observe diffraction pattern of these compounds.

CHAPTER 1

Organic pollutants in waste water

During recent years, the presence of pharmaceutical organic pollutants in the environment has become a subject of public concern. This is because of the specific biological and health effects caused by these compounds.[1] Due to the variety and amounts of usage of pharmaceuticals, they are considered to be environmentally relevant compounds.[2, 3] Some of the pharmaceutical compounds are not completely metabolized by the human body after ingestion. They enter into the municipal waste water streams unaltered or as metabolites. Even though the current concentration levels of these chemicals are low (ng L^{-1} to µg L^{-1}), continuous input and incomplete removal can be a potential risk for living organisms.[4] Compounds with a longer half-lives accumulate in the environment since they have lesser rates of removal than accumulation.[5] It is important to understand the fate and removal of these compounds from the environment, because they are potential contributors for pollution in the environment. Various studies have been done on controlling pollution caused by these compounds. A standard process for removal of organic pollutants is not possible because a wide variety of substances enter into this category.[6] Various advanced techniques have been introduced to remove a wide range of pollutants in an efficient manner.[7] This includes ozonolysis, UV photolysis, membrane bio-reaction and photocatalytic degradation. Photocatalytic degradation is an emerging technique that is effective in the removal of a wide range of compounds by simple and cost effective means.

1.1 Medical wastes: Iodinated X-ray contrast media (ICM, Scheme 1.1) are used in human medicine for imaging of organ tissues and blood vessels during diagnostic tests.

Iodine atoms are present in these compounds because they absorb X-rays.[9] ICM are applied at high doses (i.e., up to 200 g/application) and are eliminated unmetabolized in the urine within 24 h.[10] ICM are the most widely used medical waste for intravascular administration in terms of mass.[11] Annual worldwide consumption of ICM is approximately 3.5×10^6 kg.[12] It has been reported in several studies that these hydrophilic and metabolically stable ICM are not effectively removed in conventional wastewater treatment plants.[13] There is a need to find alternative techniques for removal of these compounds from waste water.

Scheme 1.1. X-ray contrast media: (**1**) diatrizoic acid, 3,5-bis(acetylamino)-2,4,6-triiodobenzoic acid, and (**2**) iohexol, 1-N,3-N-bis(2,3-dihydroxypropyl)-5-[N-(2,3-dihydroxypropyl)acetamido]-2,4,6-triiodo-benzene-1,3-dicarboxamide).

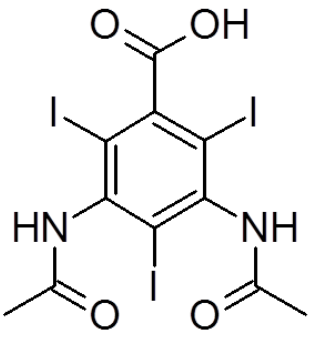

1

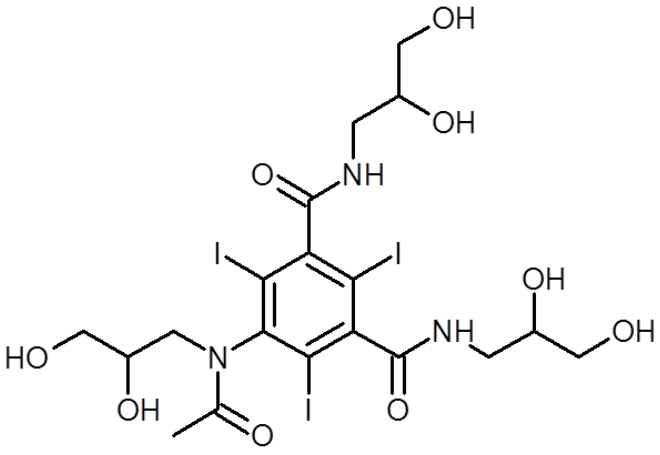

2

1.2 Surface run-off wastes: Some of the pollutants entering into waste water stream have no specific point of origin. This includes road run-off which is known to contain polycyclic aromatic hydrocarbons (PAHs).[14] Because of expansion of urban areas there has been a rapid increase in the pollution problems caused by these non-point sources of pollution.[15]Agricultural land run-off waste includes pesticides like atrazine.

1.2.1 Polycyclic aromatic hydrocarbons: PAHs are considered as persistent organic chemicals present in the environment. They are categorized as priority hazardous substances according to Water Framework Directive and Convention on Long-Range Transboundary Air Pollution of the United Nations Economic Commission for Europe (UN ECE) because of their toxic nature.[15, 16] PAHs are usually produced from vehicle exhaust emissions, vehicle tires, asphalt pavement, paint markers and on road dust.[17]

1.2.2 Triclosan: Triclosan, commercially available as irgasan, is a broad spectrum antimicrobial agent that acts against bacteria, virus and fungus.[18] It is widely used as an antimicrobial agent in personal care products at levels of up to 2% (w/w).[19] It is added in pharmaceutical products such as disinfecting soaps, medical skin creams, and dental products. It is found in everyday hygiene products such as soaps, toothpastes and mouthwashes and is also present in household cleaners, carpets and textiles, such as sportswear, shoes and bed clothes. Because of its high antimicrobial effectiveness and its easy processibility in solutions and solids, the popularity of triclosan has continuously increased over the last 30 years. This increased popularity is also because of successful marketing and increasing acceptance and desire for hygiene products by the public.[20]

Influent wastewater concentrations of triclosan are found to be as high as 4,700 ng L^{-1}.[21] Despite passing through primary and secondary treatment processes in waste water plants, its concentration in waste water effluents is found to be in the range of 42-213 ng L^{-1} resulting in the concentrations of 11-98 ng L^{-1} in the receiving rivers.[20]

Because of wide usage of this antimicrobial agent, it has been categorized as an emerging contaminant.[22]

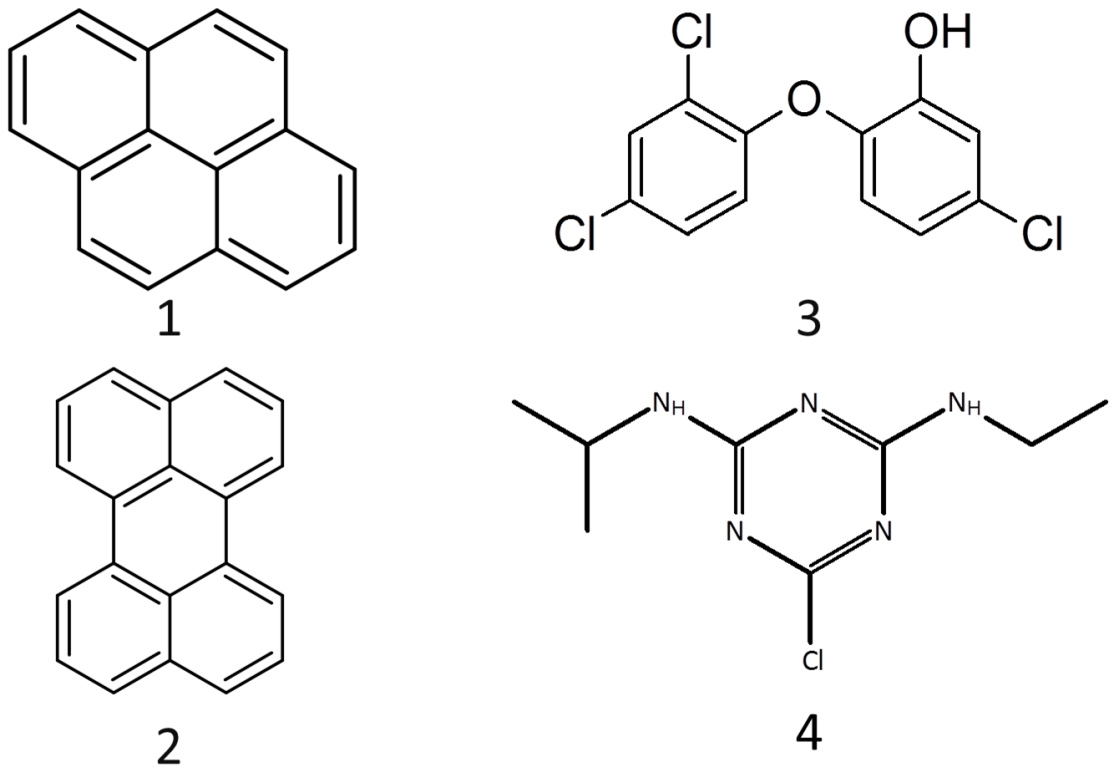

Scheme 1.2. Polycyclic aromatic hydrocarbons: (**1**) pyrene and (**2**) perylene, Antimicrobial agent: (**3**) Triclosan- 5-chloro-2-(2, 4-dichlorophenoxy) phenol and pesticide: (4) Atrazine- 1-Chloro-3-ethylamino-5-isopropylamino-2, 4, 6-triazine.

Triclosan and its degradation products have been found to be associated with long term adverse effects on aquatic life and found to have endocrine-disrupting effects in mammals.[24]

1.2.3 Atrazine: The use of agricultural pesticides throughout the world has increased rapidly during recent years, resulting in increasing concern about the environmental fate of these substances. Their usage has caused some very serious ecological concerns in terms of toxicity and pollution of water.[25] Intense investigations are being done in order to understand their ecological behavior and effect on human health before their application. Atrazine [2-chloro-4-(ethylamino)-6-isopropylamino-*s*-triazine] is an

effective herbicide for the control of annual broadleaf and some grass weeds, primarily for cultivation of maize.[26] It has been extensively used worldwide since its introduction in 1958. The half-life of atrazine (1.0 mg kg^{-1}) in the surface of soil is estimated to be 77-101 days and over 900 days in the subsurface soil.[27] Due to its widespread use and longer half-life the herbicide has been detected in many environmental compartments, especially in surface water as a result of run off following application and in drainage networks.[28]

Exposure of atrazine to humans has been suggested to result in estrogen mediated toxicities and inappropriate sexual differentiation.[29] Upon direct exposure to a UV source, it has been found that organic compounds having amine linkages such as sulfamethoxazole are susceptible to degradation, whereas compounds with amide bonds are more resistant to photodegradation.[30] The residues of many pesticides and their degradation products are now present at higher levels in the environment. Concentrations of atrazine are above normal levels of sustenance because of their relatively slow rate of natural decomposition.[25, 26]

1.3 Conventional treatment process: Municipal wastewater treatment plants are designed to eliminate biological and chemical pollutants from sewage water and prevent transfer the treated water into the aquatic environments or supply to the public.[31, 32] Several studies have been conducted on the performance of wastewater treatment plants for complete removal of pollutants.[33] It has been found that these processes are not completely eliminating organic pollutants.[34] During the wastewater treatment process most of the organic pollutants have high stability and poor biodegradability resulting detection of organic chemicals in both waste water treatment effluents and sewage sludge in considerable amounts.[35]

1.4 Advanced techniques: Implementation of novel and improved cost-effective techniques for wastewater treatment is required because of the growing incidence of hazardous pollutants over discharge limits. So, new advanced options based on catalytic processes point at being an important goal in wastewater treatments with lower organic contents, especially the so called advanced oxidation processes (AOPs).[36, 37] AOPs are considered as one of the most effective treatments for wastewater containing pollutants that are difficult to remove biologically.[38] These are found to degrade many toxic and biologically resistant organic pollutants in aqueous solution without producing additional by-products which can be more hazardous.[39] These processes are mainly based on the generation of strongly oxidizing hydroxyl radicals, which could oxidize a broad range of organic pollutants that are present in wastewater.[40] Membrane bio-reactors utilize the technology of membrane separation combined with the sludge treatment process, improving efficiency and reducing time. This works on the same principle as the conventional sludge treatment process. The difference is there is no need to perform separate filtration as in the conventional method. Low pressure microfiltration or ultrafiltration is done to separate the sludge. [41]

1.5 Photocatalytic degradation on TiO_2: The principle of photocatalytic degradation is the photoexcitation of a solid semiconductor photocatalyst as a result of the absorption of radiation, most often, but not always, in the near ultraviolet spectrum.[42] Under near ultraviolet radiation it is feasible for the semiconductor material to be excited by high energy photons producing valence band holes because of movement of conduction band electrons.[43] For TiO_2 photocatalyst, a wavelength of less than or equal to 380 nm is used to produce excited-state electron and hole pairs (Figure 1.1).[44] These charge carriers are

capable of inducing reduction or oxidation, respectively, and reacting with both water and organic compounds.[45] The holes are considered as extreme oxidants and should thus be capable of oxidizing almost all chemicals, as well as water, resulting in the formation of hydroxyl radicals and superoxide radical.[46] These radicals can then oxidize organic compounds by interacting with them.[47]

1.6 Titanium dioxide crystalline structure: The two major crystalline forms of TiO_2 are anatase and rutile and both have tetragonal structures (Figure 1.2). The common rutile surfaces (110), (100), and (001) and anatase surfaces (101), (001), and (100) lead to a large number of possible interfaces. The most stable rutile surface is the (110) surface. Besides the (110) surface, other surfaces are common and computational work indicates a surface stability order of (110) > (100) > (011) > (001). A variety of surface reconstructions are known to occur under specific conditions.[48] Surface properties of a photocatalyst may play a major role in the adsorption and subsequent charge transfer to molecules. The surface properties are not only polymorph dependent but may differ largely for the same material for different surface orientations or reconstructions.[49] This consequently contributes to the observation of pronounced surface effects in activities.[50]

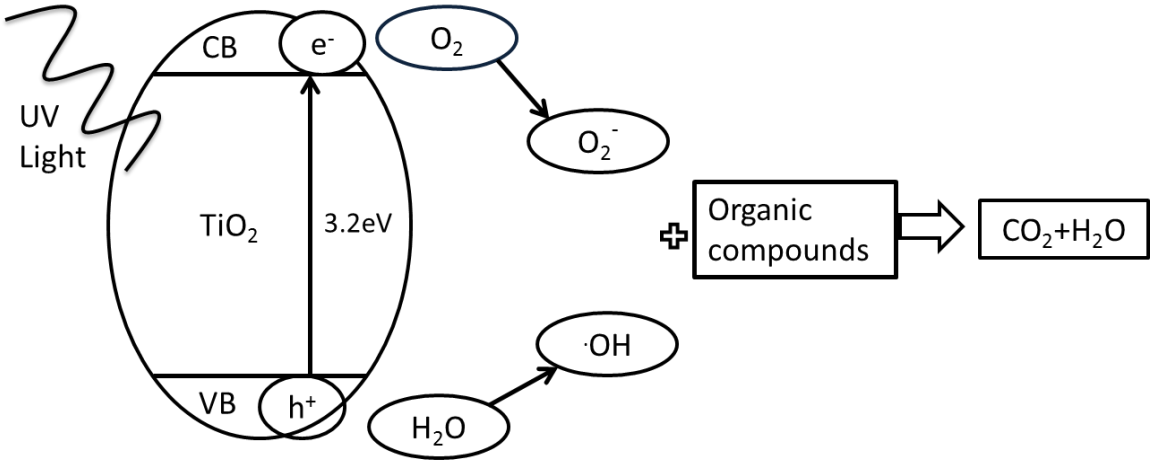

Figure 1.1. Mechanism of photocatalytic degradation. Titanium dioxide (TiO_2) absorbs ultraviolet (UV) radiation; it will produce pairs of electrons and holes. Holes can directly oxidize organic compounds. The positive holes on the surface of titanium dioxide splits water molecules to form hydroxyl radical. The negative electron reacts with oxygen molecule to form superoxide anion. Hydroxyl radical and superoxide anion react with organic compounds to ultimately produce CO_2 and H_2O.

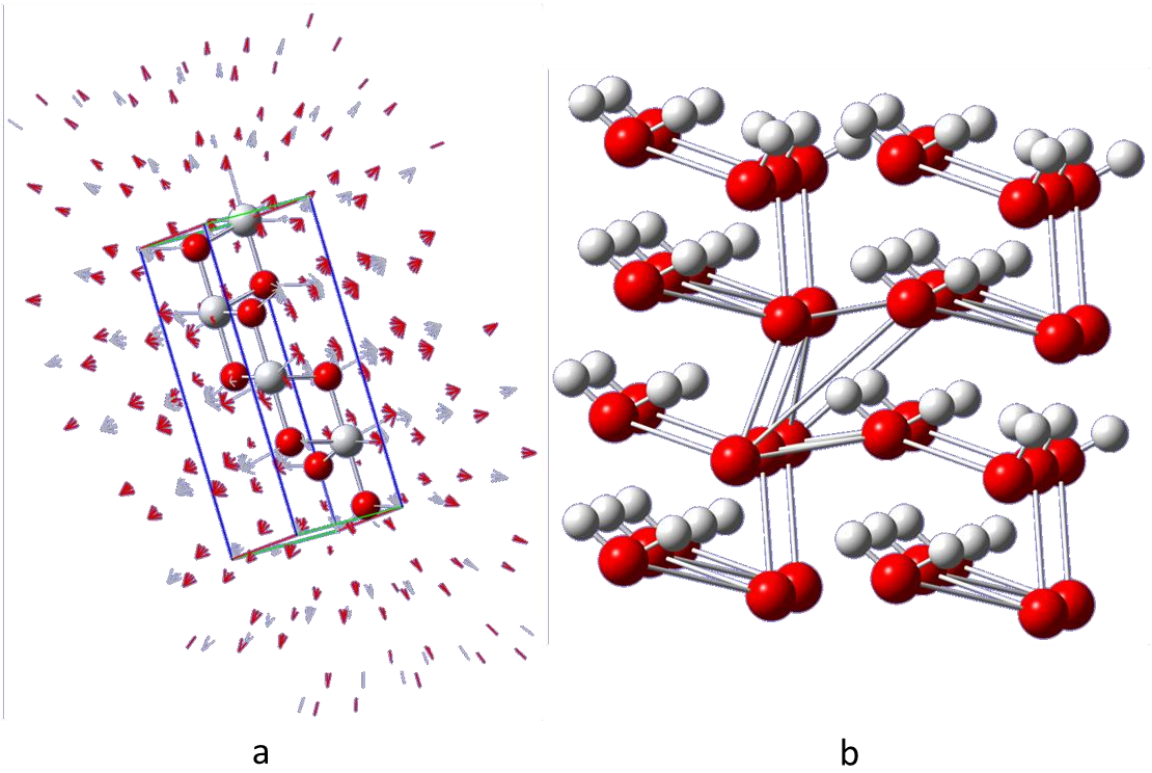

Figure 1.2. Anatase (a) unit cell. Gray and red spheres are Ti and O atoms, respectively: Rutile (b) unit cell, red and gray spheres are Ti and O atoms, respectively.

CHAPTER 2

Experimental Methods

Different classes of compounds under study as mentioned in Chapter 1 are among the most common organic pollutants found in wastewater. Titanium dioxide was obtained in two different crystalline forms (anatase and rutile). ICM include iohexol, which is a non-ionic compound, and diatrizoate, which is an ionic compound. PAHs studied were pyrene and perylene. Also studied are the most commonly used anti-microbial agent, triclosan, and atrazine, a widely used pesticide. Different methods were used to study adsorption characteristics on titanium dioxide, including thermogravimetric analysis (TGA), differential scanning calorimetry (DSC) and powder X-ray diffraction (XRD).

2.1 Materials and Reagents: All the chemicals were of reagent grade and used without any further purification. Iohexol, sodium diatrizoate, pyrene, perylene, triclosan and two different forms of titanium dioxide (anatase and rutile) were purchased from Sigma-Aldrich Co. The chemical structures of all the compounds under study are shown in Scheme 1.1 and Scheme 1.2. Sodium diatrizoate is available only in the form of a polyhydrate. The number of water molecules associated with this compound in hydrated form cannot be determined accurately. So, the solution concentrations mentioned for this compound may not be precise. Because of the higher molar mass of diatrizoate when compared with that of the lower mass of clathrate hydrate waters concentrations mentioned for this compound should be correct within 10%. This compound may be converted into anhydrate form by removing water molecules from the structure with the aid of heat before making a solution. This is not undertaken because it is not expected to affect significantly our binding results.

2.2 Experimental Procedures: Simple and reliable experimental procedures were followed for the entire work. Because of differences in solubility of the compounds in water, organic solvents such as acetone were used for PAHs and atrazine. Methanol was used for triclosan. To maintain uniformity and for best comparison of results, similar concentrations were used for all of the compounds. Solutions of organic compounds were prepared by dissolving in suitable solvent and TiO_2 was added slowly while stirring. After one hour, TiO_2 was collected for analysis.

2.2.1 Medical wastes: Three different concentrations (0.2, 0.5 and 1.0 M) of iohexol and diatrizoate were prepared by dissolving in 18-MΩ deionized water to a final volume of 10 mL. 250 mg of TiO_2 was added to these solutions slowly while stirring using a magnetic stirrer. These suspensions were stirred continuously for one hour to allow analyte to adsorb onto the surface of the photocatalyst. Then, suspensions were filtered using 45-µm Whatman nitrate cellulose membrane filters. The retenant on the surface of the filter was collected and dried. The dried sample was used for analysis using different instrumental techniques. Blanks for the analysis were prepared by using TiO_2 in same manner without addition of the analyte.

2.2.2 Run-off wastes: 0.4 M solutions of pyrene, perylene and atrazine were prepared by dissolving in acetone to a final volume of 10 mL. 250 mg of TiO_2 was added slowly to each of these solutions while stirring using a magnetic stirrer. These suspensions were continuously stirred for one hour to ensure analyte adsorption onto the surface of the photocatalyst. These solutions were dried at room temperature after removing clear supernatant solution of analytes. Sediment at the bottom was washed several times with the solvent in order to separate analyte which was not adsorbed. Blanks for the

experiment were prepared by treating TiO_2 in the same manner without addition of the analyte. 0.5 M solution of triclosan was prepared by dissolving in 99.9% methanol to a final volume of 10 mL. 250 mg of TiO_2 was added slowly to each of these solutions while stirring using a magnetic stirrer. These suspensions were dried at room temperature after removing clear supernatent of analytes. Blanks for the experiment were prepared by treating TiO_2 in the same manner without addition of the analyte.

2.3 Instrumentation: Instruments including TGA, DSC and powder XRD were used for this study. The techniques used are fast, reliable and employ small amounts of samples for analysis. Standard operating procedures according to the manufacturer of the instrument were followed for all the experiments. Instruments were periodically verified using appropriate standards to check performance and consistency.

2.3.1 TGA: Thermogravimetric analysis is widely used to study thermal properties such as thermal degradation, boiling point and desorption temperature of analytes. The TA Instruments 2950 thermogravimetric analyzer was used for all thermogravimetric analysis in the Western Kentucky University Thermal Analysis Lab. This device allows temperature measurements up to 1000 ºC. A platinum sample pan was used for analysis because it is suitable for the range of temperature studied. The sample pan was first heated over a flame in order to avoid possible contamination because only one pan was used for multiple trials. To maintain an inert atmosphere throughout analysis, the sample furnace was purged with nitrogen gas at flow rate of 60 mL/min. The balance was purged with nitrogen gas at an additional flow rate of 40 mL/min. Calcium oxalate monohydrate was used for verification of the instrument. For each measurement, approximately 10 mg of sample was loaded for analysis. The temperature was ramped at 20 ºC min^{-1} after 30

min of thermal equilibration at 36.5 ºC. All samples were analysed three times to confirm results. Thermogravimetric analysis was conducted to find out the amount of organic compound adsorbed to TiO_2, which occurs as weight loss corresponding to desorption.

2.3.2 DSC: TA Instruments differential scanning calorimeter (DSC-2920) at the Western Kentucky University Thermal Analysis Lab was used for all calorimetric studies. This device allows temperature measurements up to 550 ºC. Calorimetric studies were conducted to find out the binding energy associated with each of the compounds on TiO_2. For each measurement, approximately 10 mg of sample was loaded for analysis. Temperature was ramped at 10 ºC min^{-1} after 30 min of thermal equilibration at 25 ºC. The instrument was purged with nitrogen gas at a flow rate of 50 mL/min during analysis. This created an inert atmosphere during analysis. Standard methods for calibration were performed according to guidelines provided by the manufacturer of the instrument. Indium was used for calibration. Aluminum standard pans with a sample size of ~10 mg were used for our analysis because of range of temperature studied. These pans can be used in different ways such as open pan, closed pan, pin hole pan or sealed pan depending upon the type of sample used for analysis. Closed pans were used for this analysis. The closed pan consists of two components: bottom pan and lid. For best results, the sample was uniformly spread on the bottom pan and most of the sample was in contact with the pan. This improved thermal contact between sample and pan.

2.3.3 Powder XRD: The Western Kentucky University Rigaku Miniflex-II was used for all powder X-ray diffraction studies. Diffraction studies were conducted to examine the crystalline nature of organic compounds on TiO_2. Any change in diffraction pattern can

be observed when binding is associated with structural changes occurring in TiO_2. The sample was first ground into fine particles using a mortar and pestle. Glass slides were used for mounting of the sample. Powdered sample was mounted on the glass plate using the smear mount method. Powdered sample was spread evenly on the glass slide using methanol, which later evaporates leaving a fine layer of sample fixed on the glass slide. This glass slide was inserted into the sample cell holder of the instrument. Analysis was done over a range of 5-80° 2θ for all the samples. Diffraction patterns were obtained as intensity in counts per second as a function of 2θ which is commonly known as a diffractogram, where two theta is the scattering angle.

CHAPTER 3

Medical wastes

Several studies have been done by other researchers to study mechanisms of photocatalytic degradation of organic wastes, which occurs either through direct oxidation by holes or by indirect oxidation by radical messengers.[51, 52] Iohexol and diatrizoate do not undergo photocatalysis to the same extent, implying that direct oxidation by surface electron holes may be a major route for one compound but not the other.[53] The mechanism of photocatalytic degradation depends upon whether analyte is adsorbed on to the surface of the photocatalyst or not.[54] We performed thermal analysis on two of the most widely used iodinated contrast agents (iohexol and diatrizoate) to study their adsorption properties on titanium dioxide.

3.1 Diatrizoate and Iohexol: The DTG curve (differential thermogram) of diatrizoate is shown in Figure 3.1. The upper panel shows percentage weight of the sample as a function of temperature up to 1000 ºC. The weight of the sample is represented as percentage weight of sample taking initial weight as 100% weight on the scale. Mass loss upon increasing temperature will be interpreted as percentage weight loss of sample. The lower panel is taken as a function of derivative weight loss of sample in Derivative Mass Loss (%/ ºC). Peaks in the lower panel are observed at temperatures at which weight loss occurs in the sample.

DTG curves of iohexol and diatrizoate analytes are given in Figure 3.2. The thermal properties of compounds such as thermal degradation and evaporation are seen. All DTG curves are taken as derivative of weight loss as a function of temperature which is shown up to temperature of 1000 ºC

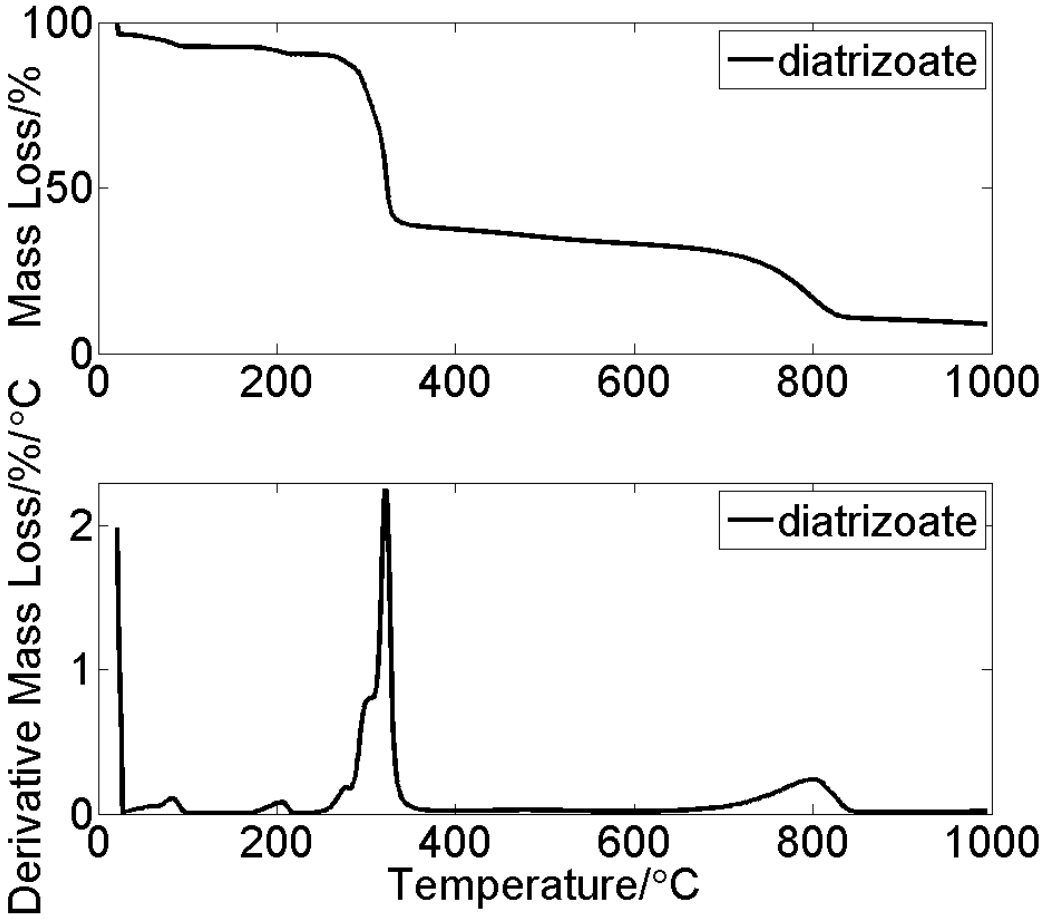

Figure 3.1. DTG curves of diatrizoate showing the temperature scale upto 1000 ºC. Upper panel is total weight percentage as a function of temperature. The lower panel shows derivative weight loss of the sample, where peaks indicate temperatures at which mass loss occurs.

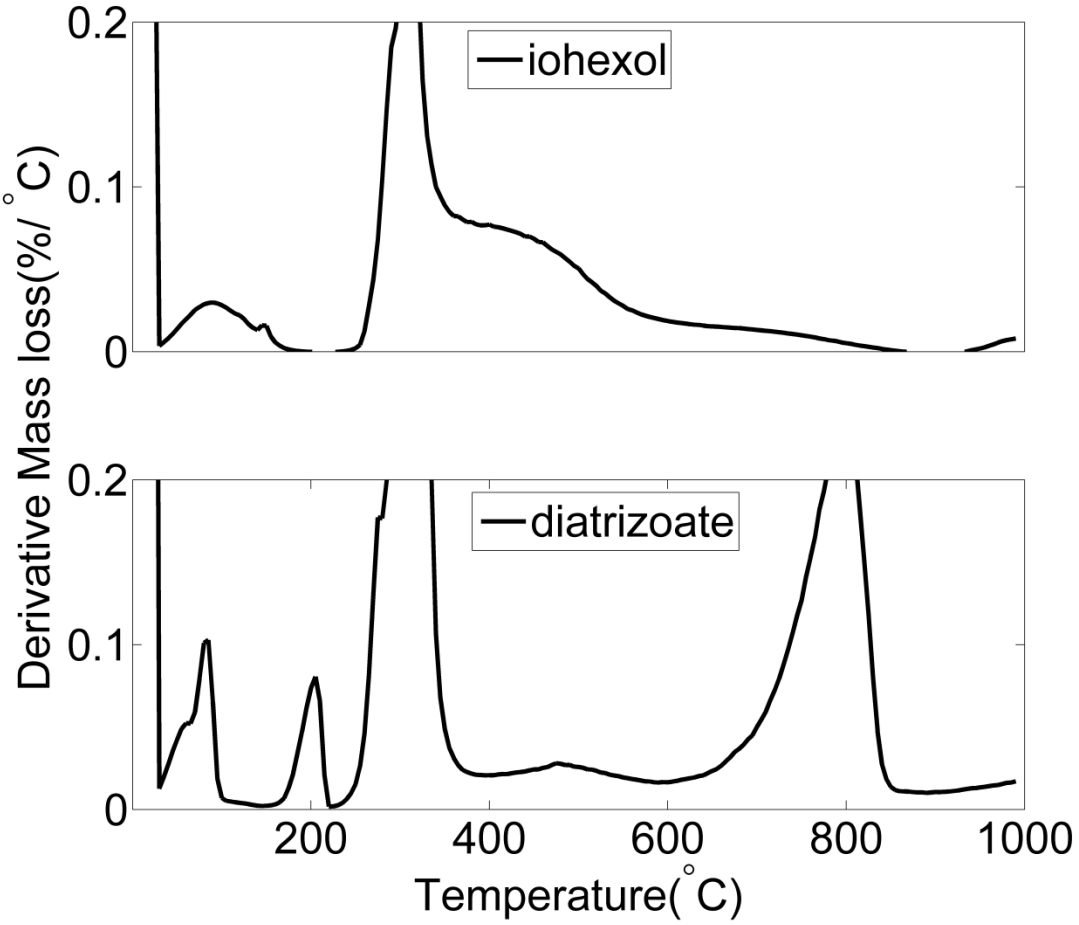

Figure 3.2. DTG curves of iohexol and diatrizoate analytes showing removal of external moisture (near 100 ºC), crystalline water (clathrates, seen in diatrizoate at 200 ºC) and physical properties such as thermal degradation (both near 300 ºC) and evaporation (diatrizoate at 800 ºC).

Table 3.1 shows the summary of DTG curves of iohexol and diatrizoate in the presence and absence of TiO_2. The first peak for iohexol represents weight loss around 100 ºC, corresponding to removal of moisture from the sample. The second peak for iohexol represents weight loss of nearly half of the remaining mass, around 300 ºC, corresponding to thermal degradation of iohexol. The first peak in the DTG curve for diatrizoate represents removal of water present as moisture around 100 ºC. The second peak is due to release of water molecules from clathrate structure of diatrizoate. The third peak is because of thermal degradation of diatrizoate.[55] Evaporation of diatrizoate is seen near a temperature of 800 ºC. The peaks from these curves are summarized in Table 3.1. Temperature ranges are characterized by both the range of the maximum derivative mass loss observed in individual experiments and by the full-width-half-maximum (FWHM) of the peak.

Table 3.1 shows a summary of thermal properties of all organic compounds under study. Desorption temperature is a function of the binding energy of analyte to the surface of photocatalyst. Iohexol and diatrizoate shows comparable desorption temperatures, which implies a similar binding pattern for the two compounds.

DTG curves for iohexol and diatrizoate in the presence of TiO_2 are shown in Figure 3.3. This reveals adsorption characteristics of the analytes onto the surface of the photocatalyst. The blank is a DTG curve of TiO_2 without addition of any analyte. No remarkable peaks are observed in the blank, indicating the absence of significant mass loss occurring in TiO_2.[56]

Table 3.1. Summary of DTG curves of iohexol and diatrizoate in the presence and absence of TiO_2. Removal of moisture for all compounds and water loss from pure diatrizoate crystal are not included. The range of peak locations given (T_{max}) is over three runs, in order to allow comparison from one run to other. Average peak full-width at half-maximum (FWHM) are provided along with assignments.

Compound Name	T_{max}/ºC	FWHM/ºC	Assignment
Iohexol	303.8-316.0	11.0	Degradation
Iohexol/Anatase	315.0-317.1	13.4	Degradation
	691.0-725.7	90.7	Desorption
Diatrizoate	320.0-321.6	11.0	Degradation
	800.0-818.6	88.4	Evaporation
Diatrizoate/Anatase	292.5-302.0	32.8	Degradation
	549.5-715.0	78.6	Desorption
	674.2-855.3	67.7	Evaporation

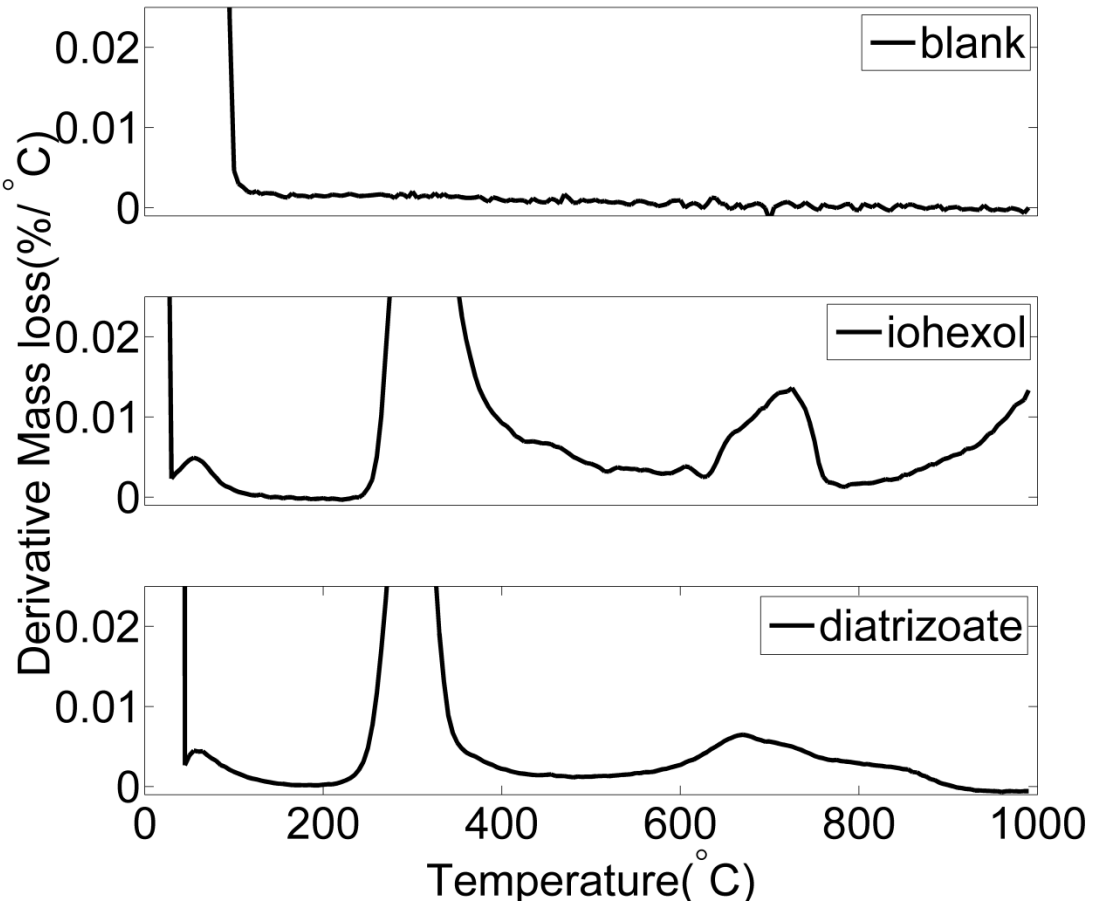

Figure 3.3. DTG curves of TiO_2 (anatase) with adsorbed analyte. The blank shows no peaks. 0.5-M iohexol and 0.5-M diatrizoate analytes show similar peaks to pure analyte at 300 ºC, but also peaks from 600-900 ºC indicating desorption off of TiO_2.

0.2-M solutions has shown correspondingly smaller peaks (meaning that the smaller peaks were lost to the noise). 1-M concentration solutions has shown nearly same results as shown for 0.5-M solutions. Thus, the substrate was completely saturated by 0.5-M solutions. No significant changes in thermal degradation or evaporation are observed for analyte in the presence of substrate when compared to pure analyte and pure substrate. The peak around 200 ºC for pure diatrizoate was not observed in the presence of substrate when compared to pure analyte. Since the analyte adsorption onto the surface of photocatalyst is no longer in the form of a crystal retaining water molecules.

In DTG curves significant changes are observed for analyte in the presence of substrate when compared to pure analyte. This is shown by the appearance of additional peaks around 725 ºC for iohexol and 670 ºC for diatrizoate. This additional peak corresponds to weight loss observed only in the presence of TiO_2. We interpret desorption of analytes from the surface of TiO_2 as the origin of these peaks.

Powder X-ray diffraction was conducted on all the compounds in order to determine the change in TiO_2 upon adsorption of analytes to on the photocatalyst. Diffractograms of iohexol in the presence and absence of TiO_2 are shown in Figure 3.4. The top panel indicates the diffraction pattern for analyte iohexol without addition of TiO_2. No distinguishable peaks are observed because of poor crystalline properties of iohexol. The slight slope in the baseline is because of the microcrystalline form of analyte. The center panel is for TiO_2 only which is consistent with those found in the literature.[57] The lower panel shows the diffractogram of TiO_2 in the presence of iohexol. Not all the peaks are observed as in middle panel for TiO_2, because they are dominated by the diffraction pattern of amorphous iohexol present on the surface of TiO_2.

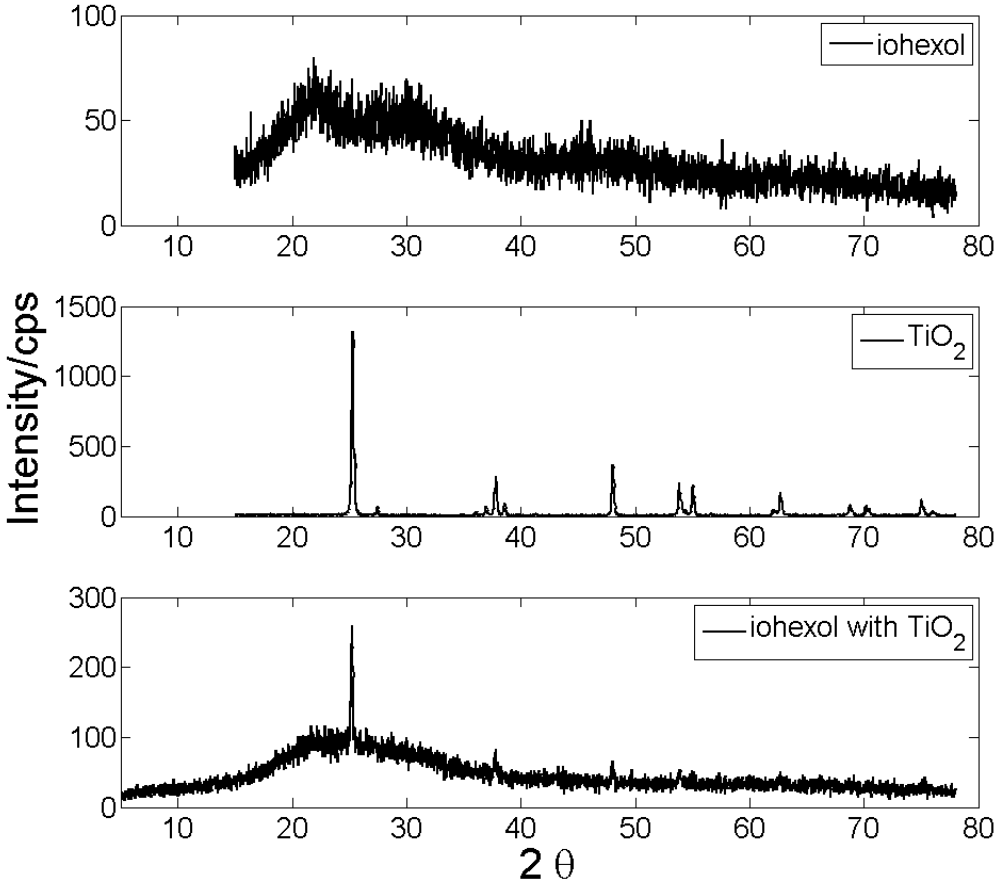

Figure 3.4. Powder XRD of iohexol. Upper panel indicates the diffraction pattern for analyte iohexol. Middle panel indicates diffraction of anatase titanium dioxide. No additional peaks are observed implying no change occurring to TiO_2.

No additional peaks are observed when compared to TiO_2, except a small rise in the baseline characteristic of the microcrystalline form of iohexol present on TiO_2.

Figure 3.5 shows the diffractogram of diatrizoate with TiO_2. As represented in the top panel for diatrizoate, a definite diffraction pattern is observed because of the presence of a crystalline form of the compound. The center panel is for TiO_2 only, which is again consistent with the previous results.[57] The lower panel shows diatrizoate in the presence of TiO_2. No additional peaks are observed when compared to TiO_2, because of the absence of significant changes in crystalline form of TiO_2.

As shown in Scheme 1.1, iohexol and diatrizoate have side chains which could have resulted in equal chances of binding to surface of TiO_2. The point of contact of the analyte molecule to the substrate is important in the process of photocatalytic degradation because oxidation through holes starts at the point of contact. Because of this binding pattern, TiO_2 primarily oxidizes side chains in ICM, leaving behind much stable aromatic ring.[53] Our binding data implies that primary degradation in both iohexol and diatrizoate could occur by direct oxidation by an electron hole at the surface of TiO_2 rather than by hydroxyl radical attack.

3.2 Effect of TiO_2 crystalline structure: TiO_2 exists in two catalytically active crystal structures, anatase and rutile. We compare structural effects of TiO_2 with the same experiments using the rutile form of TiO_2 rather than anatase. DTG curves for the rutile form of TiO_2 with and without the analyte are shown in Figure 3.6. To bring uniformity, the scales used are the same when compared to the anatase results shown in Figure 3.3. The blank indicates substrate without addition of analyte. The blank photocatalyst shows no significant peaks, nor do the samples containing analyte along with TiO_2.

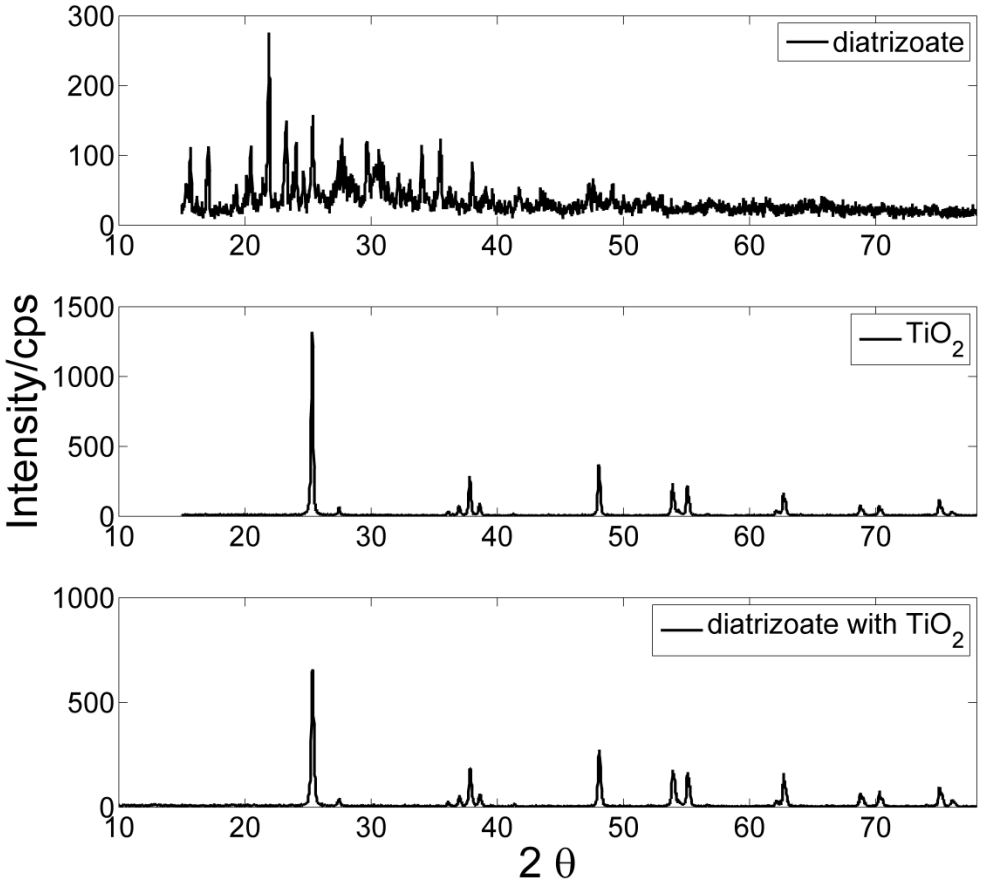

Figure 3.5. Powder XRD of diatrizoate. Upper panel indicates diffraction pattern for analyte. Middle panel indicates diffraction of titanium dioxide. No additional peaks are observed in the lower panel indicating absence of availability crystalline form of analyte.

This implies that iohexol and diatrizoate experience poor adsorption on rutile when compared with anatase. This suggests that rutile not only shows poor photocatalytic degradation of analytes in general when compared to anatase but also shows poor adsorption characteristics particularly for iohexol and diatrizoate. Lower adsorption on rutile form is associated with the higher surface energy of the crystal structure when compared to the rutile form.

As both the compounds iohexol and diatrizoate adsorb equally well on to the surface of anatase form of TiO_2, they can both possibly undergo oxidation through holes. Structural similarity between these two compounds might have resulted in comparable binding energies implying binding could occur in same manner for both of the compounds.

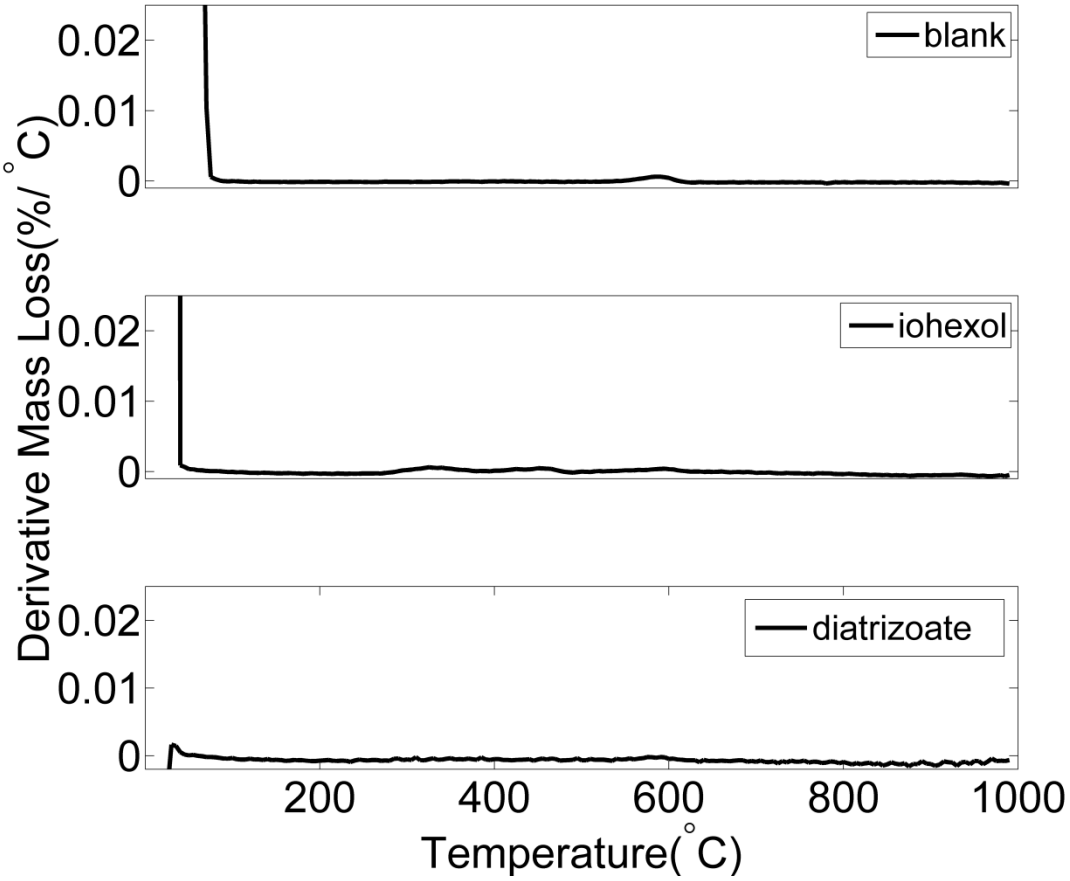

Figure 3.6. DTG curves of TiO_2 (rutile) with iohexol and diatrizoate. In contrast to the anatase form, no peaks are seen because of no effective adsorption.

CHAPTER 4

Surface run-off wastes

Organic compounds which do not have specific points of origin are non-point sources of pollution. Thermal analysis was conducted on three different classes of organic compounds found in surface run-off water. The first class includes PAHs, namely pyrene and perylene. The second class includes an antimicrobial agent, triclosan. The third class, pesticides, was represented by atrazine. These three classes of organic compounds have different aromatic ring structures, which may or may not have side chains.

4.1 Polycyclic aromatic hydrocarbons: The investigation on mechanism and degradation products during photocatalytic degradation of PAHs has been conducted in organic solvents in the presence of semiconductor photocatalyst because of poor solubility in aqueous solutions.[58] Several researchers have discussed about the photocatalytic oxidation products to understand fate of these compounds during degradation.[59] One of the main degradation pathways for PAHs occurring in the natural aquatic environment is through oxidation. Previous studies have indicated that the main oxidation reaction for PAHs is the interaction with superoxide radical (O_2^-) resulting in the formation of more water-soluble oxidized compounds or into smaller degraded organic molecules. Exact degradation products of PAHs depend on the chemical nature of the parent compound.[60]

As described in the methods section, suspensions of analytes on photocatalysts were prepared using acetone as solvent because these are water insoluble compounds. DTG curves for pyrene and perylene are shown in Figure 4.1. The first peak for pyrene

represents weight loss around 250 ºC, this corresponds to thermal degradation of pyrene.[61] Thermal degradation of perylene is seen at 300 ºC. Table 4.1 shows the thermal properties and desorption temperatures of the analytes. DTG curves for pyrene and perylene in the presence of TiO_2 are shown in Figure 4.2. As before, the blank is for TiO_2 without the addition of pyrene and perylene. No significant peaks are observed, suggesting the absence of any weight loss occurring in TiO_2. In the DTG curves of pyrene in the presence of TiO_2, no additional peaks were observed when compared to the blank, implying effectively no adsorption to the surface of photocatalyst. Perylene with its similar structural formula to pyrene, shows similar results. Perylene's peak around 300 ºC is seen in the presence of TiO_2 is presumed to be because of the presence of perylene that is not adsorbed on TiO_2. Unadsorbed analyte is present because of incomplete washing of the TiO_2.

Table 4.1. Experimental thermal properties of analytes and desorption temperatures from TiO_2 obtained using thermogravimetric analysis.

Analyte	Thermal degradation (ºC)	Evaporation (ºC)	Desorption temperature (ºC)
Pyrene	250	-	-
Perylene	350	-	-
Triclosan	-	250	400
Atrazine	-	220	370

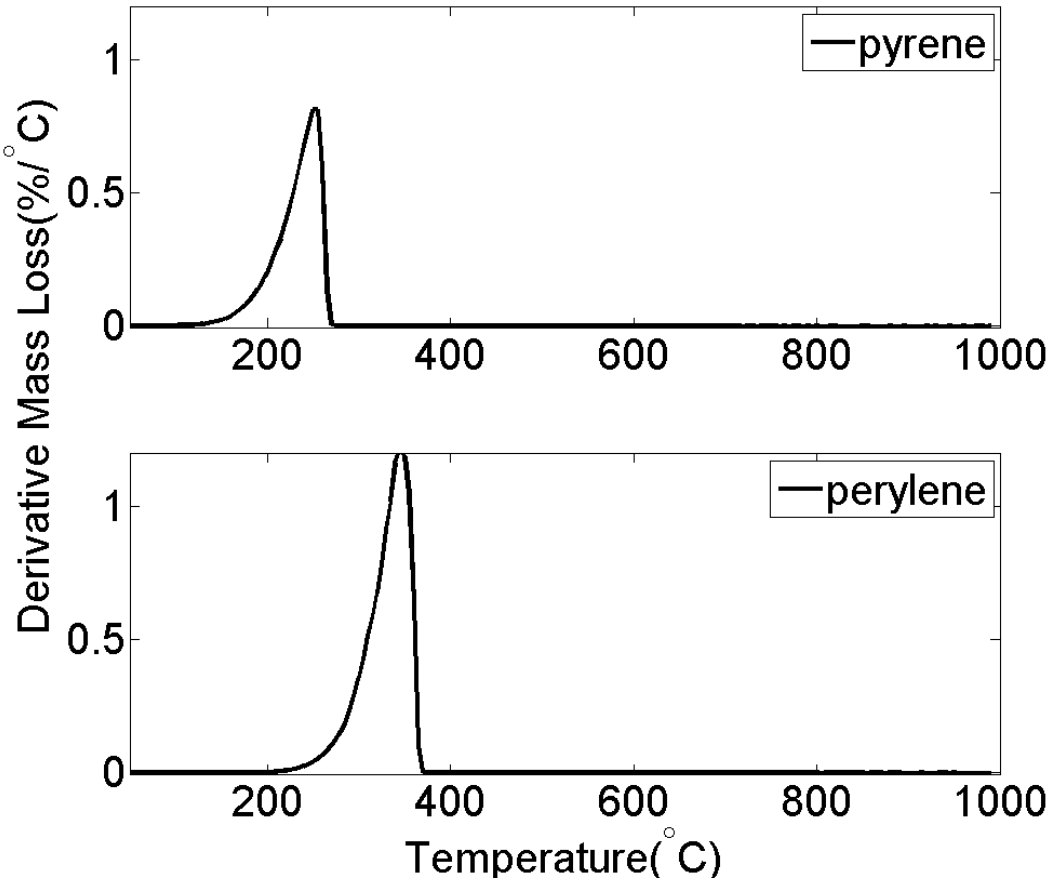

Figure 4.1. DTG curves of pyrene and perylene analytes showing thermal degradation near 250 ºC and 350 ºC.

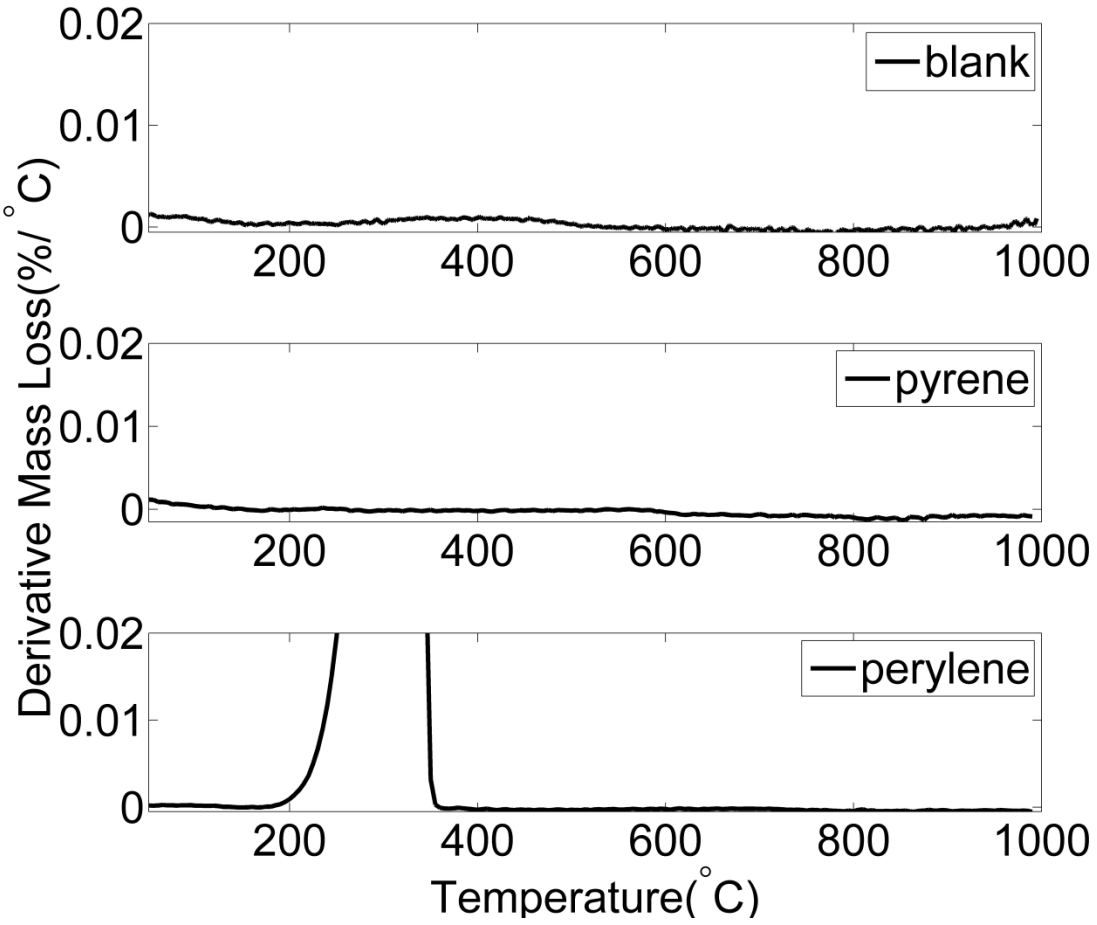

Figure 4.2. DTG curves of TiO_2 (anatase) with adsorbed analyte. The blank and pyrene show no peaks. For perylene, no additional peaks are seen except for thermal degradation of un-adsorbed perylene.

The powder X-ray diffraction pattern for pyrene is shown in Figure 4.3. The top panel indicates the diffractogram of pyrene without TiO_2. Peaks observed are characteristic of the crystalline form of the compound. Center panel is for the diffraction pattern of TiO_2 only which is consistent with the previous results.[57] The lower panel is for pyrene in the presence of TiO_2. No additional peaks are observed when compared to TiO_2, because of the absence of the crystalline form of analyte on the photocatalyst.

The diffractograms of perylene in the presence and absence of TiO_2 are shown in Figure 4.4. The top panel indicates the diffraction pattern for analyte perylene without addition of TiO_2. Distinguishable peaks observed indicate the presence of the crystalline form of analyte. The center panel is for TiO_2 only which is consistent with the previous results.[57] The lower panel is the diffractogram of perylene in the presence of TiO_2. Additional peaks appear at the same locations as pure perylene when compared to just TiO_2. This is characteristic of the presence of crystalline form of perylene along with, but not adsorbed onto the TiO_2.

As stated in the previous chapter, adsorption of analyte to the surface of the photocatalyst is required for direct oxidation through electron holes. Our results suggest that pyrene and perylene do not effectively adsorb onto the surface of TiO_2. These compounds do not have side chains, which may make them less able to adsorb on to the surface of TiO_2. Even though TiO_2 is considered to form covalent and ionic bonds with analytes, it is not effective in binding anthracene derivatives lacking side chains. These compounds may undergo photocatalytic degradation through hydroxyl radical attack rather than direct oxidation through holes. These radicals introduce hydroxyl and carbonyl groups into the ring system.[62, 63]

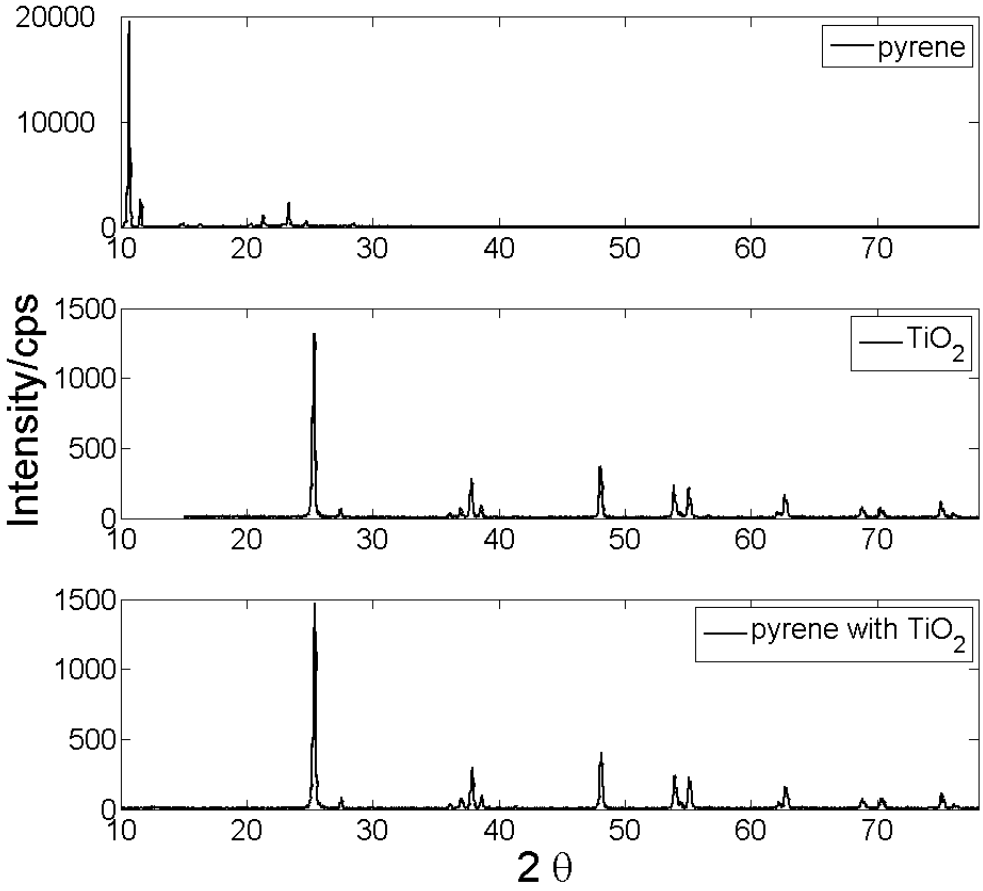

Figure 4.3. Powder XRD of pyrene. Upper panel indicates the diffraction pattern for the analyte. Middle panel indicates the diffraction of titanium dioxide. No additional peaks are observed in the lower panel indicating the absence of significant amounts of availability of the crystalline form of analyte.

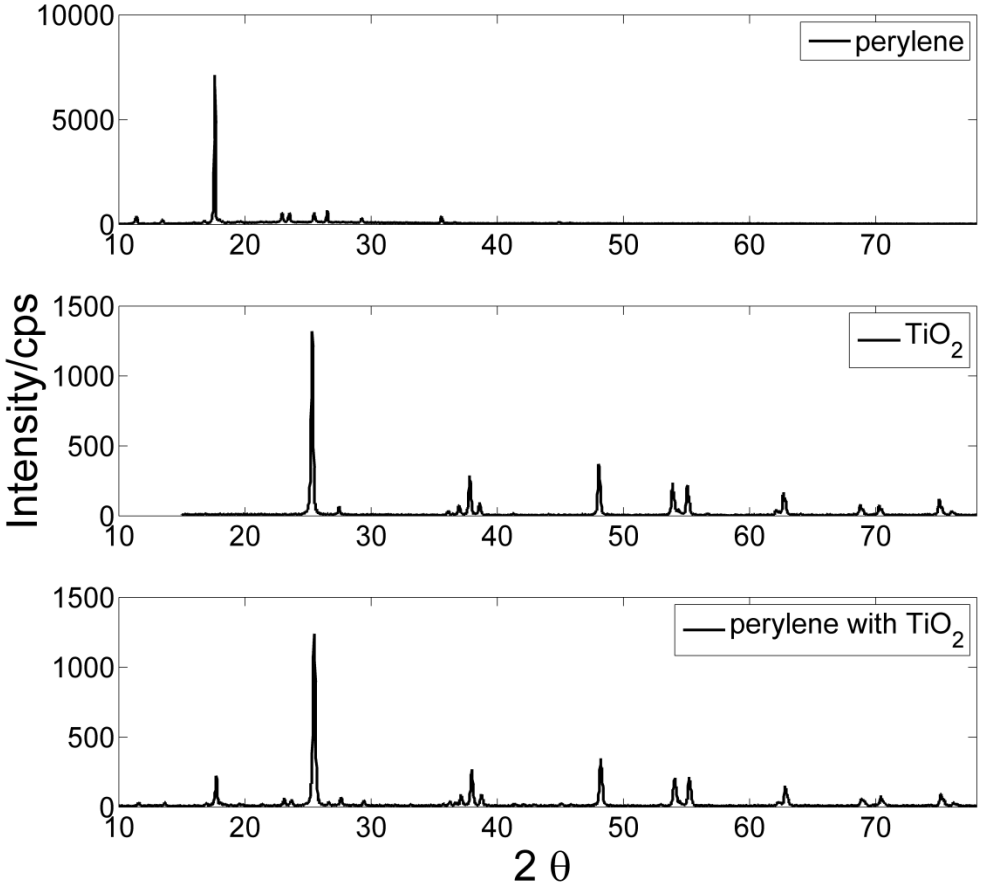

Figure 4.4. Powder XRD of perylene. Upper panel indicates the diffraction pattern for analyte. Middle panel indicates the diffraction of titanium dioxide. Additional peaks are observed in the lower panel indicating availability crystalline form of analyte.

Several compounds, such as 1, 6-pyrene-dione and 1, 8-pyrene-dione, have been suggested as initial pyrene photochemical products.[62]

4.2 Triclosan: The structure of the broad spectrum antimicrobial agent triclosan was shown in Scheme 1.2. The presence of triclosan and its transformation products in the aquatic environment is of great concern because of its harmful degradation intermediates. Harmful photocatalytic degradation products of triclosan include chlorinated phenols, chlorohydroxydiphenyl ethers, 2,7- and 2,8-dichlorodibenzo-p-dioxin, and a possible dichlorodibenzodioxin isomer or dichlorohydroxydibenzofuran.[64, 65]

The DTG curves for triclosan without TiO_2 is shown in Figure 4.5 to reveal physical properties of the analyte such as evaporation. Table 4.1 shows the thermal properties and desorption temperature of this analyte. The first peak for triclosan represents weight loss around 200 ºC corresponding to the evaporation of the triclosan.[66] The blank is the DTG curve of TiO_2 without addition of triclosan. The lower panel is the DTG curve of triclosan in the presence of TiO_2, which, like diatrizoate and iohexol, shows an additional peak compared to just triclosan and just TiO_2 around 400 ºC.

Differential scanning calorimetry (DSC) is conducted in addition to TGA because the desorption temperature obtained using TGA is lower than 500 ºC. Using the WKU DSC instrument one can reach upto temperatures of 500 ºC. DSC is used to find the reaction process occurring in the sample is either endothermic or exothermic, based on the sign of the peak appearing on the temperature scale.

An endothermic peak is a result of heat absorbed by the sample, forming a peak below the baseline. An exothermic peak is a result of heat released by the sample, forming a peak above the baseline.

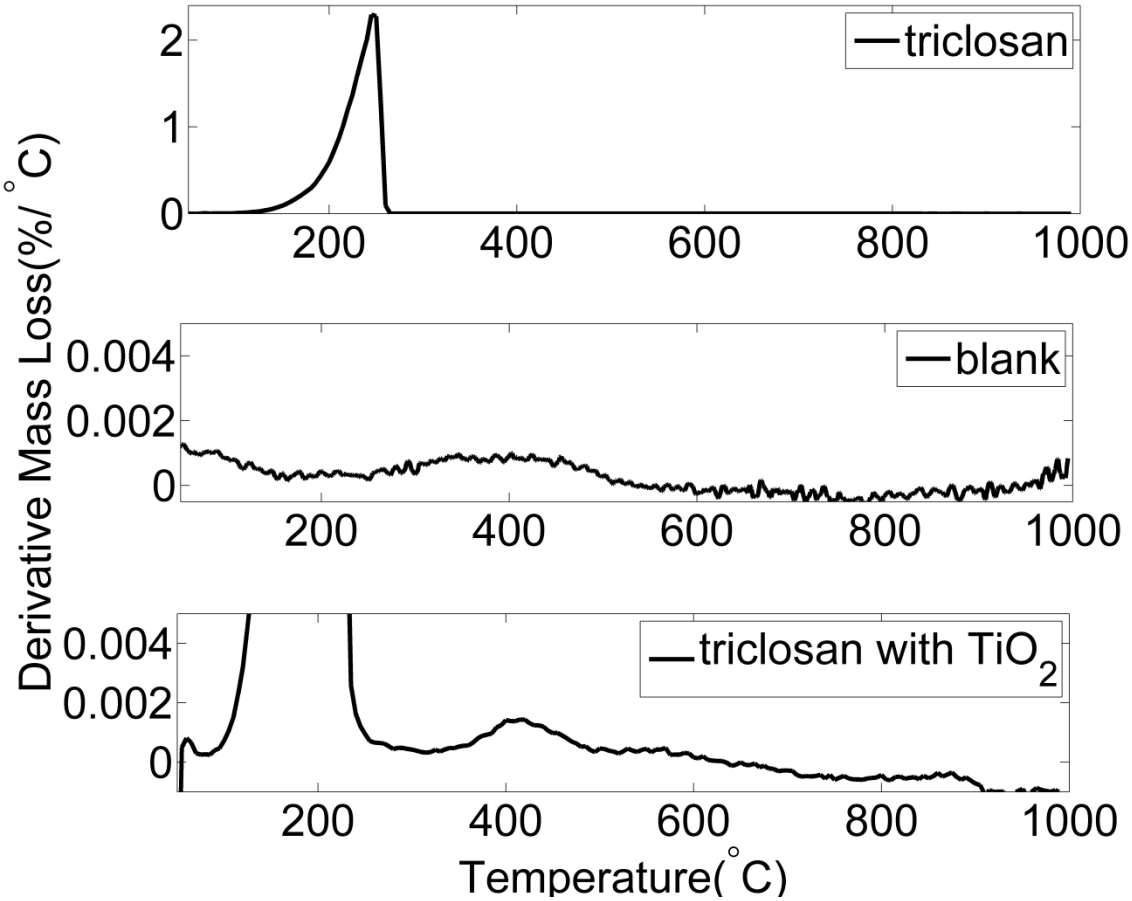

Figure 4.5. TG curves of analyte triclosan. Peak at 250 ºC is because of evaporation of analyte. Blank TiO_2 shows no peaks. Additional peak around 400 ºC in the presence of TiO_2 indicate desorption of analyte.

DSC curves for triclosan are shown in Figure 4.6. The top panel shows triclosan without TiO_2. The first endothermic peak corresponds to the melting point of triclosan and the second endothermic peak is for the evaporation of triclosan. The center panel is for TiO_2 only. The absence of any significant peaks indicates no phase changes occurring in TiO_2 over the temperature range. The bottom panel shows triclosan in the presence of TiO_2. No significant change in melting point was observed when compared to pure analyte. The additional peak at 100 ºC corresponds to the boiling point of water. An exothermic peak is obtained around 470 ºC. The process of desorption of analyte from the substrate should result in the formation of an endothermic peak. The appearance of an exothermic peak may be because of rearrangement of TiO_2 occurring during desorption of analyte from substrate.

Table 4.2 includes summary of DSC data of analytes triclosan and atrazine. DSC curves as mentioned above gives the melting point, boiling point and desorption for these two analytes. It is confirmed from our results that triclosan adsorbs well on the surface of TiO_2. Thus, triclosan can possibly undergo direct oxidation through electron holes.

Figure 4.7 shows the diffractogram of triclosan with TiO_2. As represented in the top panel for triclosan, no peaks are observed because of the absence of the crystalline form of the compound. The slight slope in the baseline is because of the microcrystalline form of the analyte. The center panel is for TiO_2 only, which is consistent with the previous results.[57] The lower panel shows triclosan in the presence of TiO_2. Unlike in the other compounds, additional peaks are observed in the bottom when compared to TiO_2, which might be a result of rearrangement occurring in TiO_2 structure, similar to rutile.

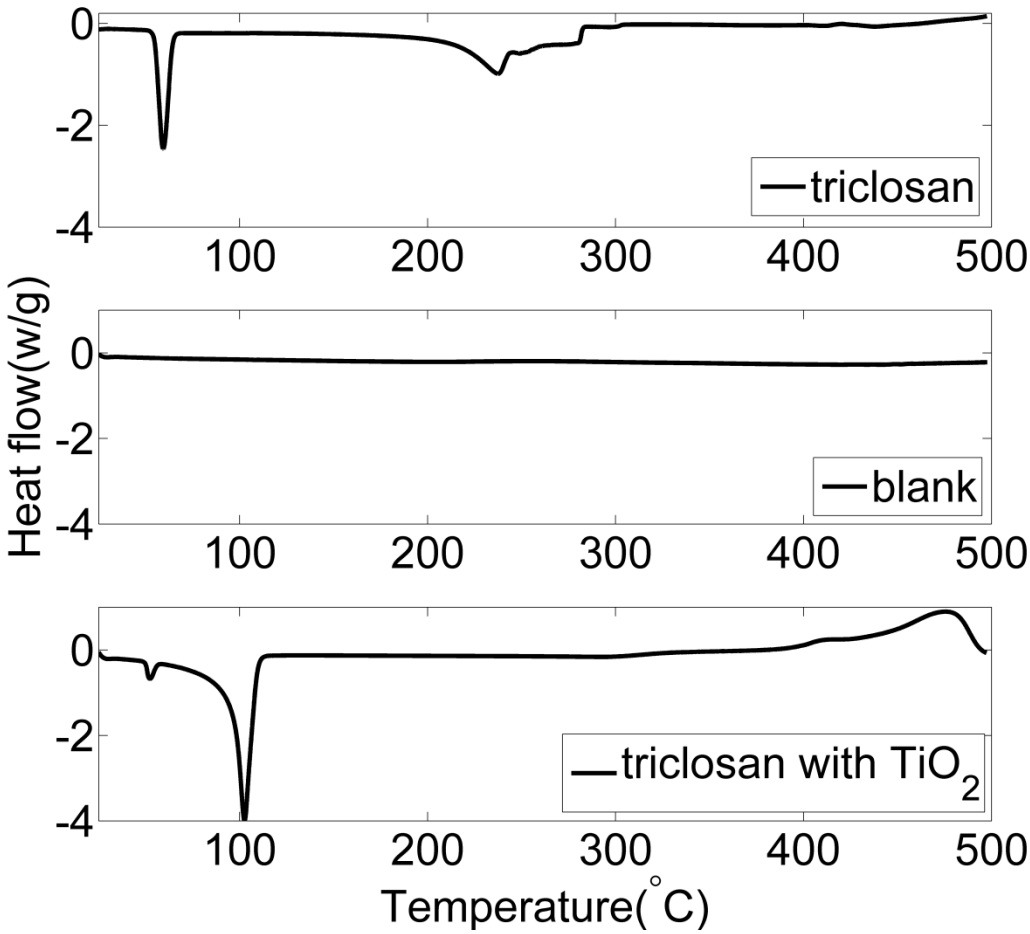

Figure 4.6. DSC curves of TiO_2 (anatase) with triclosan. Peak at 60 ºC corresponds to melting point of analyte. Peak at 250 ºC is because of boiling of analyte. Blank shows no structural changes. Additional peaks in the presence of TiO_2 indicate desorption. Appearance of an exotherm during desorption is associated with rearrangement occuring of TiO_2.

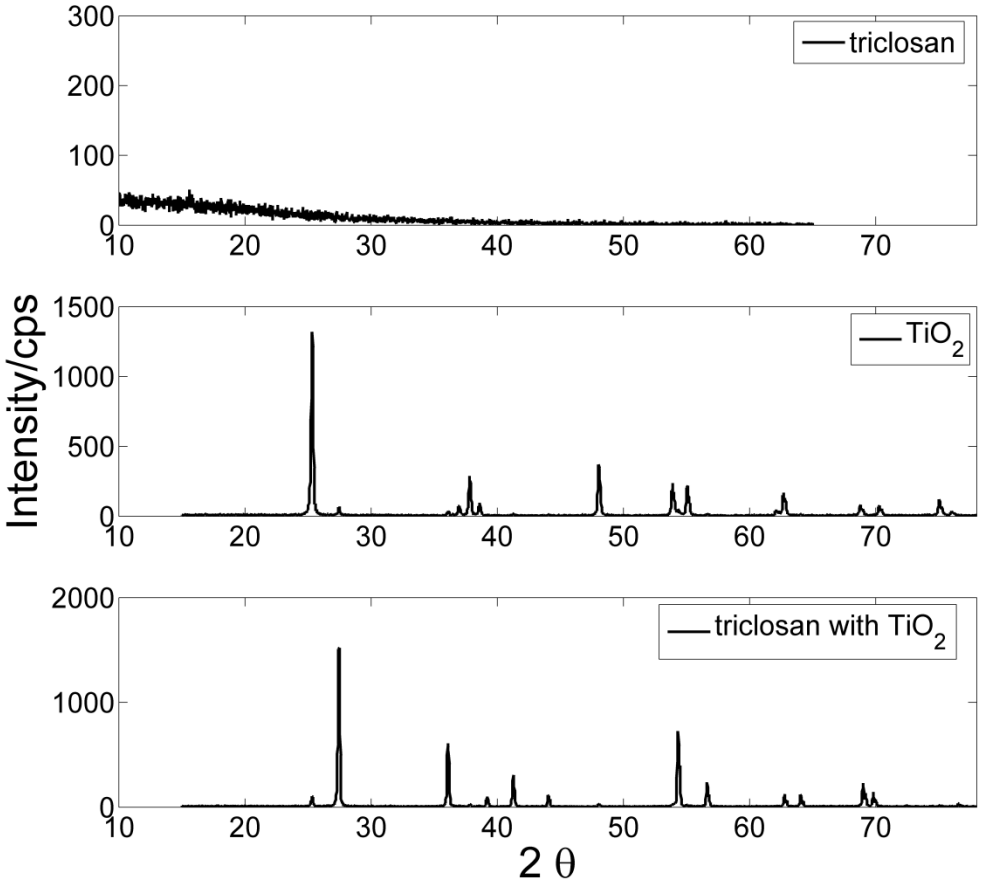

Figure 4.7. XRD curves of triclosan on TiO_2 shows additional peaks because of presence of rearrangement occurring in titanium dioxide.

Table 4.2. Experimental thermal properties of analytes and desorption temperatures from TiO_2 obtained from differential scanning calorimetry.

Analyte	Melting point(ºC)	Boiling point(ºC)	Desorption temperature(ºC)
Triclosan	60	240	470
Atrazine	180	250	370

Changes to the TiO_2 structure could also have implications for photocatalytic degradation. Future work will be to confirm this hypothesis by analysis using GSAS software to convert the diffractogram to a structure.

4.3 Atrazine: The structure of the pesticide atrazine is shown in Scheme 1.5. Upon direct exposure to UV source, it has been found that organic compounds having amine linkages such as sulfamethoxazole are susceptible to degradation, whereas compounds with amide bonds are more resistant to photodegradation.[30] Thus, atrazine is also sensitive to photodegradation since it also has amine groups. Degradation of atrazine forms a stable compound cyanuric acid, reducing the number of carbon atoms from eight to three. During photocatalytic degradation partial removal of the carbon atoms within the atrazine side chains forms five carbon compounds during the degradation pathway including deisopropylatrazine, 2-hydroxydesisopropyl atrazine and 2-hydroxy-4-acetamido-6-amino-1, 3, 5-triazine.[67]

DTG curves for atrazine and TiO_2 are shown in Figure 4.8. The top panel indicates the DTG curve of atrazine, to reveal physical properties of the analyte such as evaporation which occurs near 210 ºC.[68] The center panel is the DTG curve of TiO_2 only.

Lower panel is for DTG curve of atrazine in the presence of TiO_2. Atrazine on TiO_2 gives an additional peak at 375 ºC because of desorption of analyte from TiO_2. Table 4.1 shows the thermal properties of atrazine.

DSC curves for atrazine are shown in Figure 4.9. The top panel is the DSC curve of pure analyte atrazine. Analyte shows two peaks. The first peak corresponds to the melting point occurring at 175 ºC and second peak corresponds to boiling point of atrazine occurring at 250 ºC.[68] Center panel indicates DSC curve of TiO_2. The bottom panel indicates the DTG curve of atrazine on TiO_2. The additional peak at 370 ºC is the result of desorption of the compound. As for triclosan this peak is exothermic, which could be due to TiO_2 rearrangement. A summary of calorimetric studies are given in Table 4.1.

Figure 4.10. Shows diffractograms of atrazine with TiO_2. As represented in the top panel for atrazine, a definite diffraction pattern is observed for the crystalline compound. The center panel is for TiO_2 only, which is consistent with the previous results. The lower panel is for atrazine in the presence of TiO_2. No additional peaks are observed when compared to TiO_2, because of absence of crystalline form of atrazine with TiO_2. During sample preparation of atrazine with TiO_2, atrazine is present in soluble form. Here no evidence is seen to support rearrangement of TiO_2 as compared to triclosan data. No additional peaks are observed when compared to TiO_2, because of absence of crystalline form of atrazine with TiO_2. During sample preparation of atrazine with TiO_2, atrazine is present in soluble form. Here no evidence is seen to support rearrangement of TiO_2 as compared to triclosan data.

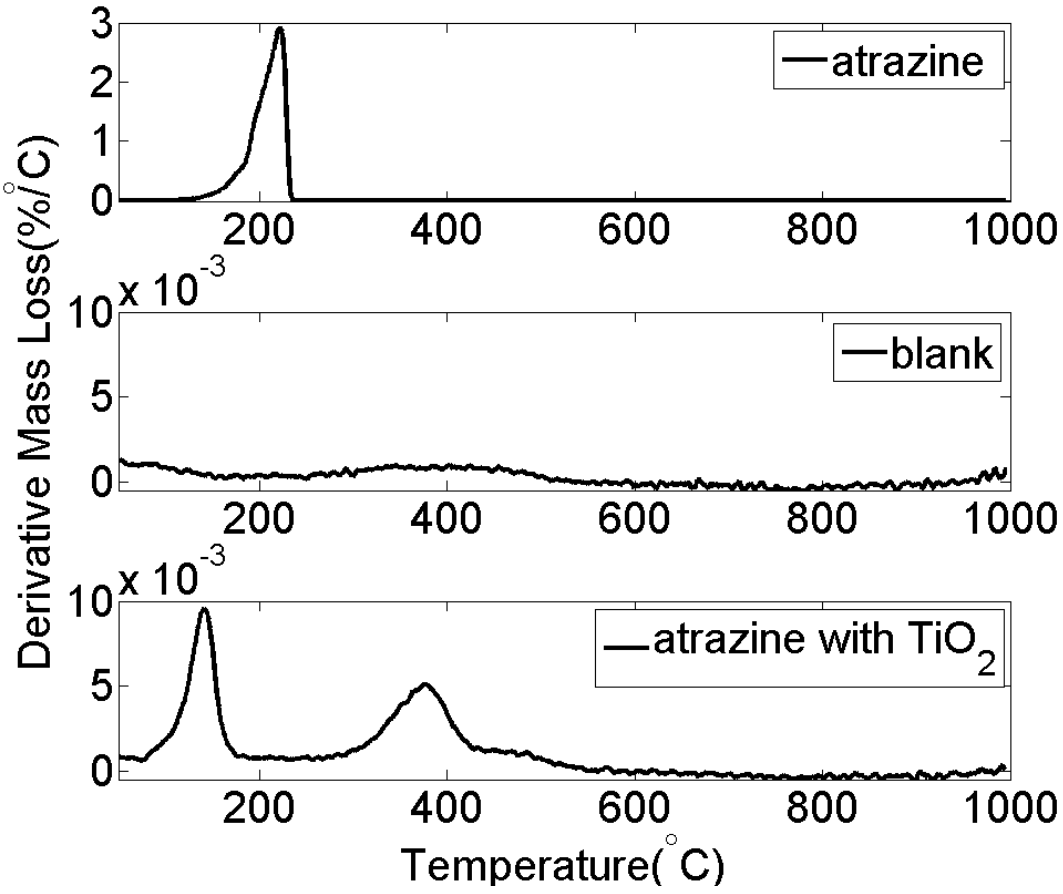

Figure 4.8. TGA curves of atrazine with and without substrate. Analyte (atrazine) at top panel shows one peak corresponding to the evaporation. The blank shown in the middle panel indicates just TiO_2 shows no peaks. Atrazine with TiO_2 shows additional one peak at 370 ºC indicating desorption.

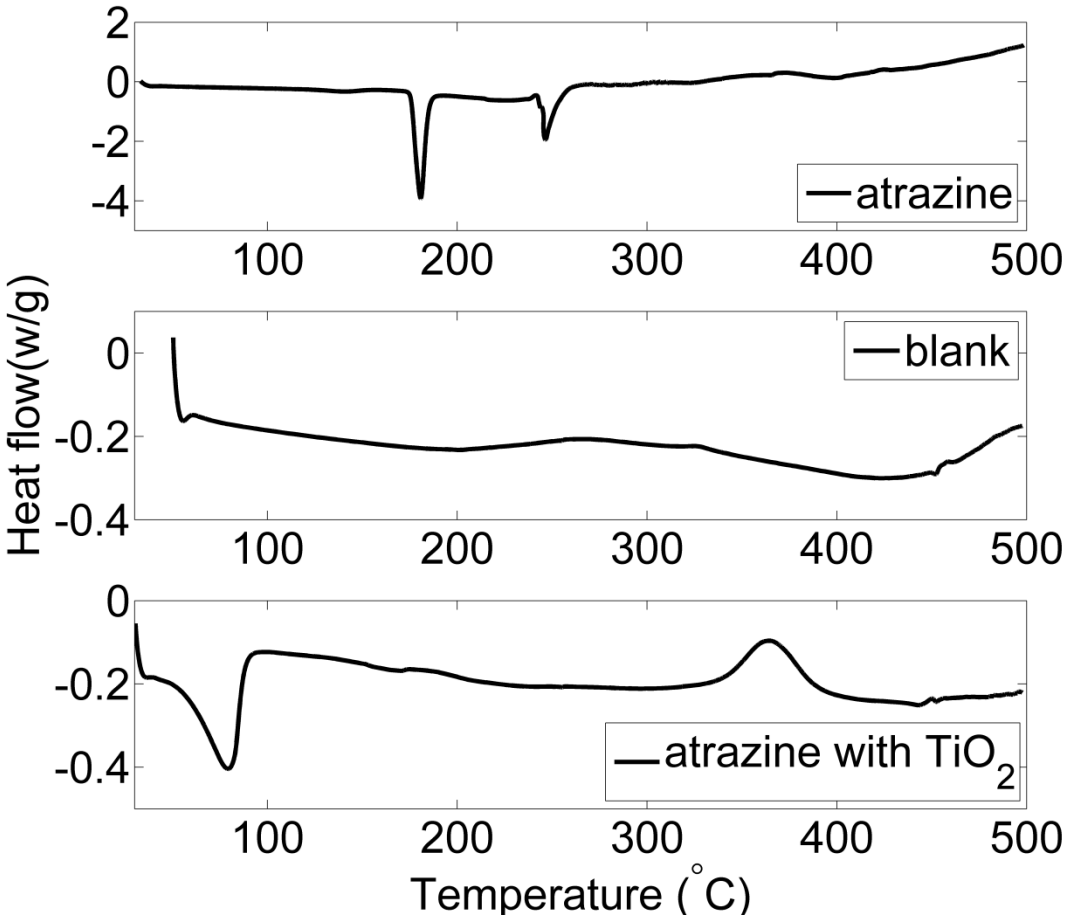

Figure 4.9. DSC curves of atrazine with and without substrate. The top panel represents atrazine, with the first peak corresponding to melting around 175 ºC; the second peak corresponds to the boiling point around 250 ºC. The middle panel represents just TiO_2. Atrazine with TiO_2 shows one additional peak at 370 ºC indicating desorption.

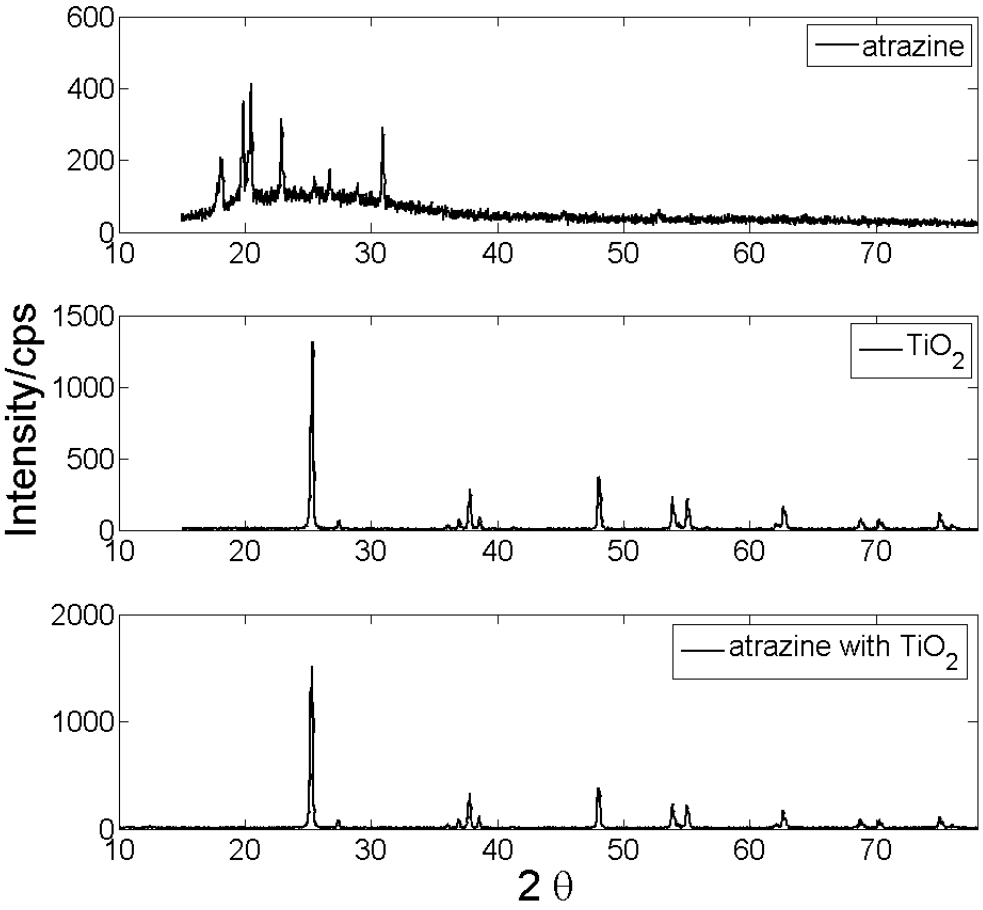

Figure 4.10. Powder XRD of atrazine. Upper panel indicates diffraction pattern for analyte. Middle panel indicates diffraction of titanium dioxide. No additional peaks are observed because of absence of crystalline form of analyte on titanium dioxide.

CHAPTER 5

Conclusions: Thermal analysis of four different of classes organic compounds on TiO_2 revealed which of the compounds can easily bind on the TiO_2. Compounds adsorbed on the photocatalyst can potentially undergo direct oxidation through holes. This extent of adsorption affects photocatalytic degradation because adsorption of a compound is necessary to undergo direct oxidation through electron holes. DTG curves of iohexol and diatrizoate reveal that both of the compounds adsorb approximately equally well onto the surface of anatase TiO_2. DTG curves of iohexol and diatrizoate with the rutile form of TiO_2 shows that this crystalline form is not suitable for binding of these compounds. We attribute this to poor adsorption of analytes to the rutile form when compared to anatase. Because of the similar binding levels on anatase (based on both percent mass loss and on the similar temperatures for desorption), we conclude that the difference of photocatalytic degradation pattern between these compounds is not because of a difference in their adsorption to TiO_2. These compounds are equally amenable to oxidation by electron holes from the surface of TiO_2 particles during a photocatalytic degradation reaction, at least from the perspective of ability to bind to TiO_2.

DTG curves of pyrene and perylene show that there are no desorption peaks for the compounds. This implies that PAHs may be minimally adsorbed on to the surface of TiO_2. Because of poor adsorption characteristics of these two compounds, they are less likely to undergo direct oxidation through electron holes. These compounds are more susceptible to undergo indirect oxidation through free radical mechanism.

DTG curves of triclosan show that an additional peak is observed for analyte in the presence of TiO_2. DSC curves shows an additional exothermic peak occurring at

similar temperature as in the DTG curve. This peak may be because of a desorption process occurring for the compound. The diffractograms for the compound shows additional peaks for TiO_2 in the presence of substrate. We interpret these as a result of rearrangement occurring in the photocatalyst during adsorption, implying that triclosan adsorbs well on the surface of TiO_2, so that this compound can potentially undergo oxidation through electron holes. Further analysis to confirm this hypothesis is needed, particularly to ensure that this is not an effect of preferred alignment.

Atrazine shows an additional peak in the DTG curve, only in the presence of TiO_2 may be because of desorption. DSC curve shows an exotherm occurring at same temperature as DTG curve. Desorption should be characterized by the appearance of an endothermic peak. This exothermic peak can be a result of rearrangement process occurring in the sample, though the diffractogram shows no additional visible spectral features for analyte in the presence of substrate. Atrazine can undergo direct oxidation through electron holes during photocatalytic degradation on TiO_2, because adsorption is necessary for compound to undergo direct oxidation through electron holes. This general approach is simple to measure, and may serve as an alternative to more complicated approaches which add foreign agents (such as oxalic acid) to the reaction.

BIBLIOGRAPHY

1. Doll, T. E. and Frimmel, F. H. *Chemosphere,* 52, **2003,** 1757-1769.

2. Halling, S. B. and Nors, N. *Chemosphere,* 36, **1998,** 357-393.

3. Ternes, T. *Water Res.,* 32, **1998,** 3245-3260.

4. Fram, M. S. and Beiltz, K. *Sci. Total Environ.,* 409, **2011,** 3409-3417.

5. Petrik, J. O. *Water Air Soil Pollut.,* 224, **2013,** 1770-1800.

6. Donnera, D. E. and Eriksson, E. C. *Sci. Total Environ.,* 408, **2010,** 2444-2451.

7. XU, J. L. *Crit. Rev. Env. Sci. Technol.,* 42, **2012,** 251-325.

8. Ternes, T. A. and Hirsch, R. *Environ. Sci. Technol.,* 34 , **2000**, 2741-2748.

9. Fram, M. S. and Beiltz, K. *Sci. Total Environ.,* 387, **2008**, 1235-1246.

10. Steger, H.T.; Leange, R.; Schweinfurth, H.; Tschampel, M. and Rehmann, I. *Water Res.,* 36, **2002,** 266-274.

11. Egeria, S. and Marika, M. *Vascul. Pharmacol.,* 58, **2013,** 48-53.

12. Namasivayam, S. M.; Kalra, M. K.; Torres, W. E. and Small, W. C. *J. Environ. Manage.,*107, **2012,** 96-101.

14. Nakada, N. H. *J. Environ. Chem,* 16, **2006,** 389-401.

15. JiJi, R. D.; Cooper, G. A.; Booksh, K. S. *Anal. Chim. Acta*, 397, **1999,** 61-72.

16. Daniele, F.; Alessandro, G. R.; Cristian, T. and Kurt, A. S. *J. Anal. Appl. Pyrolysis,* 103, **2013,** 60-67.

17. Murakami, M. N. *Chemosphere*, 61, **2005,** 783-791.

18. Bester, K. *Water Res.,* 37, **2003,** 3891-3896.

19. Sabaliunas, D. and Webb, S. *Water Res.,* 37, **2003,** 3145-3154.

20. Heinz, S. S. *Environ. Sci. Technol.,* 36, **2002,** 4998-5004.

21. Heidler, J. and Halden, R. *Chemosphere,* 66, **2007,** 362-369.

22. Anger, C. S. *Environ. Sci. Technol.,* 47, **2013,** 1833-1843.

23. Geens, T. N. *Chemosphere,* 87, **2012,** 796-802.

24. Raut, S. A. *Environ. Toxicol. Chem.,* 29, **2010,** 1287-1291.

25. Korte, F.; Konstantinova, T.; Mansour, M.; Ilieva, P. and Bogdanova, A. *Chemosphere,* 35, **1997,** 51-54.

26. Borio, O.; Gawlik, B. M.; Bellobono, I. R. and Muntau, H. *Chemosphere*, 37, **1998,** 975-989.

27. Elena, B. M. *J. Agric. Food Chem.,* 52, **2004,** 7382-7388.

28. Schottler, S. P.; Eisenreich, S. J.; and Capel, P. D. *Environ. Sci. Technol.,* 28, **1994,** 1079-1089.

29. Sanderson, J. T.; Seinen, W.; Giesy, J. P. and vanden Berg, M. *Toxicol. Sci.*, 54, **2000,** 121-127.

30. Kim, I. T. *Environ. Intern.*, 35, **2009,** 793-802.

31. Pal, A.; Gin, K. Y.; Lin, A. Y. and Reinhard, M. *Sci. Total Environ.,* 408, **2010,** 6062-6069.

32. Nakada, N.; Kiri, K.; Shinohara, H.; Harada, A.; Kuroda, K.; Takizawa, S. and Takada, H. *Environ. Sci. Technol.*, 42, **2008,** 6347-6353.

33. Nakada, N.; Tanishima, T.; Shinohara, H.; Kiri, K. and Takada, H. *Water Res.,* 40, **2006,** 3297-3303.

34. Radjenovic, J.; Petrovic, M. and Barcelo, D. *Water Res.*, 43, **2009,** 831-841.

35. McClellan, K. and Halden, R. *Water Res.,* 44, **2010,** 658-668.

36. Peranthoner, S. *Top. Catal.,* 207, **2005,** 1-4.

37. Maldonado, M. I. *J. Photochem. Photobiol. A,* 185, **2007**, 354-363.

38. Akbal, F. *Environ. Monit. Assess.,* 83, **2003,** 295-302.

39. Han, W. Y. *Catalysis Today,* 90, **2004**, 319-324.

40. Qamar, M. *J. Environ. Manage.*, 80, **2006,** 99-106.

41. Melin, T. A. *desalination*, 187, **2006,** 271-282.

42. Herrmann, J. H. *Catalysis Today,* 53, **1999,** 115-129.

43. Sixto, M.; Julian, B.; Alfanso, V. and Christoph, R. *Appl. Catal. B,* 37**, 2002,** 1-15.

44. Kormann, D. W. *Environ. Sci. Technol.*, 25, **1991,** 494-500.

45. Detlef, B. *Solar energy*, 77, **2004,** 445-459.

46. Herrmann, J. M. *J. Hazard. Mater.,* 146, **2007,** 624-629.

47. Mills, A. *Catalysis Today,* 129, **2007,** 22-28.

48. Beck, T. J.; Klust, A.; Batzill, M.; Diebold, U.; Di, V. C. and Selloni. *Phys. Rev. Lett.*, 93, **2004,** 36-104.

49. Wilson, J. N. *J. Catal.*, 214, **2003,** 46-52.

50. Wilson, J. N. *J. Amer. Chem. Soc.*, 124, **2002,** 11284-11285.

51. Yatskiv, G. V. *Theor. Exp. Chem.*, 39, **2003,** 48-52.

52. Sabina, S.; Logan, H. and Nee, M. J. *J. Raman. Spectrosc.*, 44, **2013,** 1746-1752.

53. Jeong, J. J. *Water Res.*, 44, **2010,** 4391-4398.

54. Shen, M. *Langmuir*, 27, **2011,** 9430-9438.

55. Nashwa, E. G. *Int. J. Pharm*., 391, **2010,** 305-312.

56. Zarbin, D. C. *J. Braz. Chem.*, 15, **2004,** 378-384.

57. Swanson, H. E.; and Tatge, E. *Geological*, 539, **1953**, 95-104.

58. Mackay, D. S. and Shiu, W.Y. *J. Chem. Eng. Data.*, 22, **1977,** 399-402.

59. Pagni, R. M. and Sigman, M. E. *Environ. Photochemistry*, 2, **1999,** 139-180.

60. Yu, H. *J. Environ. Sci. Health. C Environ. Carcinog. Ecotoxicol. Rev.*, 35, **2002,** 105-125.

61. Jude, A. O. *Fuel*, 85, **2006,** 75-83.

62. Reyes, C. A.; Medina, M.; Crespo-Hernandez, C.; Cedeno, M. Z.; Arce, R., Rosario, O. and Dabestani, R. *Environ. Sci. Technol*, 34, **2000,** 415-422.

63. Mazur, M. and Blanchard, G. J. *J. Phys. Chem. B*, 108, **2004,** 1038-1045.

64. Aranami, K and Readman. J. W. *Chemosphere*, 66, **2007,** 1052-1056.

65. Tixier, C.; Singer, H.; Canonica, S. and Muller, S. R. *Environ. Sci. Technol.*, 36, **2002,** 125-132.

66. Uyar, A. C. *Langmuir*, 27, **2011,** 6218–6226.

67. McMurray, T. A. and Dunlop, P. S. *J. Photochem. Photobiol.*, 182, **2006,** 43-51.

68. Dongmei, J.; Yuejin, L.; Yaping, L. and Changhai, L. *J. Chem. Eng. Data*, 58, **2013,** 3183−3189.